Development of a Cystic Fibrosis Microphysiological Model of the Kidney Proximal Tubule

Francine Celise Siqueira Cesar Carnevale

A thesis

submitted in partial fulfillment of the

requirements for the degree of

Master of Science

University of Washington

2021

Committee:

Edward J. Kelly, Chair

Yvonne Lin

Program Authorized to Offer Degree:

Pharmaceutics

University of Washington

Abstract

Development of a Cystic Fibrosis Microphysiological Model of the Kidney Proximal Tubule

Francine Celise Siqueira Cesar Carnevale

Chair of the Supervisory Committee:
Edward J. Kelly
Department of Pharmaceutics

Abstract: Cystic fibrosis (CF) is an autosomal recessive genetic disease caused by a spectrum of mutations in the cystic fibrosis transmembrane conductance regulator gene (*CFTR*), whose protein product functions as a chloride channel. The impact of CF on airway and digestive systems is well studied; however, the impact of CFTR deficiency on kidney function is not well characterized. The reasons for a lack of data on kidney function in the CF population is that, historically, patients typically succumbed to other morbidities, particularly opportunistic lung infections. With the development of new therapeutics, including inhaled antibiotics, pancreatic enzyme replacement therapy, lung transplants and, most recently, development of small molecule drug CFTR "correctors and potentiators" the lifespan of a CF patient has increased significantly to a median of 44 years in the United States, as of 2017 with the increased lifespan of CF patients, it is anticipated that they will also now be susceptible to "normal" age-related co-morbidities including chronic kidney disease (CKD), which has a prevalence of ~12% in US adults aged 45-64. A unique risk factor that CF patients face regarding CKD is repeated exposure to high dose aminoglycoside and polymyxin antibiotics for treatment of opportunistic lung

infections by gram negative bacteria. As these antibiotics are known to induce acute kidney injury, it is reasonable to predict higher than average risk of CKD in CF patient populations. Renal clearance of both antibiotic classes is believed to be mediated by endocytic uptake at the apical membrane of renal proximal tubule epithelial cells via the cubilin/megalin complex. In CF patients, it has been hypothesized that this endocytic complex in the kidney may be impaired, as "shed" cubilin has been observed in the urine of CF patients and mice lacking CFTR have decreased expression of the cubilin receptor in the kidney and low molecular weight proteinuria. Another study suggests that CF patients may be protected from polymyxin-induced acute kidney injury (AKI) relative to normal subjects. Taken together, these observations point to decreased CFTR function as conferring protection against antibiotics renally cleared by the cubilin/megalin pathway. However, with restoration of CFTR function by corrector/potentiator therapeutics, the risk of acute kidney injury and CKD is a possibility that must be considered when managing opportunistic lung infections in CF patients. **Thus, we hypothesize that individuals with CF may be protected from antibiotic-induced AKI due to impaired cubilin/megalin endocytic function in the kidney proximal tubule.** To address this hypothesis, our aim was to develop a model of CF proximal tubule epithelial cells (PTECs) using a 3D microphysiological system (MPS) cultured with cells from wild type (WT) and *CFTR* gene-edited ferrets. The rationale for using this preclinical model versus other species is that ferrets lacking CFTR exhibit a similar lung disease phenotype to humans, unlike the *CFTR* knockout mouse. We isolated, propagated, and characterized ferret PTEC (fPTEC) from ferret kidneys, and optimized the cell culture media to minimize transition from epithelial to fibroblast-like morphology. Furthermore, we established a fPTEC MPS, minimized cell aggregation and improved the epithelial morphology in 3D culture, tested for cubilin shedding in MPS effluents and evaluated endocytic function via uptake

of fluorescently labeled albumin. No cubilin shedding was detected by ELISA nor we were able to measure endocytosis of labeled albumin, but optimization of fPTEC MPS development is required. We maintained fPTEC viability of 5 days in MPS and a functional response to SGLT2 inhibition in 2D culture. In conclusion, we have a better understanding of the culture of fPTECs in 2D culture and MPS, supporting their future use in modeling CF kidney function and response(s) to antibiotic-induced AKI.

ACKNOWLEDGEMENT

Foremost, I would like to express my sincere gratitude to my advisor Prof. Edward J. Kelly for the immense support, patience, and guidance. I could not have imagined having a better advisor and mentor, and I am truly gratefully for the personal and professional growth achieved during the past 2 years of my Master`s studies.

Besides my advisor, I would like to tank Yvonne Lin on my thesis committee for the valuable feedback on my thesis.

I want to thank my fellow lab mates for the stimulating discussions and assistance, and for all the wonderful moments we had together.

I also want to thank my family and friends for all the love and care.

Finally, I am thankful for the funding support provided from P30 DK089507; Cystic Fibrosis Translational Research in the Post-CFTR Modulator Era: Pilot Program Project title: “Modeling the CF Kidney Phenotype”

Dedication

To each patient with cystic fibrosis, may we advance the science frontiers and provide a better quality of life.

Table of Contents

Table of Figures

1. INTRODUCTION

1.1 Cystic fibrosis

Cystic fibrosis (CF) is a lethal genetic disorder that affects mostly Caucasians with an incidence of 1 in 2,500 individuals (1); in 2007, there were around 35,000 cases registered in the United States and more than 70,000 people living with this condition worldwide. (2,3) The disease is caused by a plethora of mutations in the gene for the cystic fibrosis transmembrane conductance regulator (CFTR) that functions as an ATP-binding cassette (ABC) transporter expressed on the apical membrane of epithelial cells.(4) Those mutations cause an impairment of CFTR function that disturbs the electrolyte balance and results in thick secretion accumulation in multiple organs.(5)

Lung disease is the major cause of mortality in cystic fibrosis and progresses from multiple inflammations and infections that results in airway obstruction and pulmonary insufficiency, with an inevitable consequence of severe lung damage requiring lung transplantation.(6) The median survival expectancy for an individual born in 2017 in United States is 46.2 years, (7) a large increase compared to the life expectancy for a child born in the 1960s which was 5 years old. (1) This dramatic improvement in the life expectancy is attributed to the development of therapies aimed at the clearing the airways, the treatment of infections, addressing nutrition deficits, and correcting the defective CFTR proteins. (7,8)

CF is a multiorgan disease and can also impair, liver, gastrointestinal tract, and endocrine system.(9,10) In the kidney, CFTR is mainly expressed at the apical membrane of proximal tubule, but its association in CF-related kidney disease remains unknown. (11) Understanding the

role of CFTR in the kidney is an important aspect to patient care since patients are chronically exposed to some antibiotics that are nephrotoxic, and with the increase in lifespan due to the improvement of therapies, age-related comorbidity such as chronic kidney disease (CKD), is expected to surge. (10,11) CKD prevalence in 2021 in non-CF adult population aged 45-64 is approximate 12% in United Stated. (12)

Some studies (13–15) suggest that the decreased function of CFTR can confer the CF patients with a protection against antibiotics renally cleared by the cubilin/megalin pathway. However, the access to new drug therapies targeting the correction of CFTR could pose a risk of acute kidney injury (AKI) and CKD in CF patients; therefore, understanding the role of CFTR on kidney function may contribute to the therapy management in order to prevent renal toxicity.

1.2 Molecular mechanisms of cystic fibrosis

CFTR is a membrane protein with 1,480 amino acids and comprises two domains (TMD1 and TMD2) of six transmembrane α helices connected by cytosolic and extracellular loops, forming a chloride pore. CFTR, a member of the ABC transporter family, mainly allows the transport of Cl^- across the epithelium, playing a central role in transepithelial salt transportation and dynamic electrolyte equilibrium. (16) CFTR is regulated by two cytosolic nucleotide binding domains (NBD1 and NBD2) with two sites for ATP binding, and an R domain that regulates NBD1 and NBD2 through phosphorylation. The N and C termini of CFTR are intracellularly oriented (See **Figure 1**). (16)

Variants in *CFTR* by amino acid substitutions, frameshifts, splice sites and nonsense alterations can cause either malformation or loss of expression of the CFTR protein, resulting in

loss of CFTR-controlled chloride and bicarbonate balance. To date, there are more than 1,700 mutations identified in the *CFTR* gene, and the deletion of amino acid phenylalanine at codon 508, known as ΔF508, corresponds to the most prevalent alteration, being observed in 70% of the CF cases. Another mutation, G551D, has a lower frequency of 0.1%. (17)

There are six different classes of *CFTR* mutations. Class I relates to interruption of protein synthesis due to the presence of a premature stop codon, or frameshift resulting in deletions or insertions. Class II is associated with defective protein trafficking to the cell membrane due to a failure in folding and subsequent endoplasmic reticulum associated degradation. ΔF508 is an example of a Class II mutation. Class III generates channel gating defects, leading to depletion of ATP binding and subsequent protein hydrolysis. Class IV mutations result in less functional proteins, i.e., reduced chloride conductance. Class V mutations cause a decrease in the number of CFTR protein that reaches plasma membrane, while class VI mutations result in less stable proteins. (18)

1.3 Evidence of defective endocytic uptake in the proximal tubule

Various studies have shown evidence of CF patients having decreased renal toxicity after exposure to nephrotoxic antibiotics as compared to non-CF patients.(13–15) A multicenter cohort investigation evaluated adult patients with normal renal function who received polymyxin, a nephrotoxic antibiotic, in a multicenter study. They suggested that among the patients with cystic fibrosis there was a protective factor for nephrotoxicity. (13) The overall rate of kidney injury was significantly lower in patients with CF treated with polymyxin B and colistin, both nephrotoxic antibiotics, compared to the non-CF patients. (14) Similarly, no

decline was detected in GFR of CF patients exposed to 5 years high dose regimen of aminoglycosides. (15) Polymyxin and aminoglycoside antibiotics are recognized to induce nephrotoxicity through the reabsorption in the proximal tubule, which is driven by the endocytic receptors megalin and cubilin. (19–21)

Megalin is a 600 kDa single transmembrane receptor protein that belongs to the low-density lipoprotein receptor family. Cubilin is a 460 kDa peripheral membrane glycoprotein co-expressed with megalin in the apical endocytic compartments of the proximal tubule. Both proteins form a multi-receptor complex that guide internalization and reabsorption of many substances, including albumin, hormones, vitamins, and low molecular weight proteins. (19,22)

In individuals with CF compared to non-CF adults, increased cubilin is excreted in urine, as well as a 30-fold increase in the levels of urinary transferrin, a natural ligand to cubilin. It was suggested that the inactivation of CFTR leads to instability of cubilin, resulting in accelerated shedding of cubulin in the urine. (23) Additional evidence of defective endocytic uptake associated with CFTR mutation was provided in a study where the researchers genotyped patients with Dent`s disease, which is caused by mutations in the genes *CLCN5* or *OCRL* that results in low molecular weight proteinuria. The researchers found *CFTR* mutations in patients with Dent`s disease reinforcing the hypothesis of a disfunction on megalin/cubilin endocytic uptake caused by *CFTR* mutation. (24)

1.4 Cells, ferrets, and microphysiological systems in cystic fibrosis research

There is a myriad of immortalized cell lines to evaluate the impact of *CFTR* mutations in respiratory and intestinal systems, but very few choices exist for renal assessment.(25) While

established immortalized cell lines are advantageous due to their increased life spans, they fail to reproduce the heterogeneous physiology and dynamically complex biochemistry of the tissue. Cell lines rely on clones isolated from a mixed population of primary cells, with distinct phenotypic characteristics, and it is not certain that immortalized cells will carry the same phenotype of interest observed in the primary cells. (25)

Primary cell cultures, on the other hand, can reveal a more complete map of the biological heterogeneity and the metabolic dynamics associated to a complex disease such CF. The availability of primary renal cells bearing *CFTR* mutations may promote a better understanding of the impact of CF on the kidney in an experimental scenario that is more analogous to a tissue from a CF patient. CF human kidney biopsies represent the finest option to study CF renal phenotypes by providing primary cells, however access is limited. As an alternative, primary kidney cells from genetic engineered animals carrying the *CFTR* mutations represent a practical alternative. The ferret (*Mustela putorius furo*) with genetically engineered *CFTR* mutations has proven to be a useful species for modeling cystic fibrosis in the lungs, intestine, and pancreas. (26) The lungs of the CF ferrets have many aspects in common to human lungs relating to morphology and biological function. CF ferrets develop spontaneous lung infection after birth and show similar signs of lung pathology such as airway obstruction, thick mucus, and inflammation. CF ferrets can also develop a CF disease phenotype analogous to humans due to ferrets' abundance of tracheal glands dependent on Cl^- and HCO_3^- for secretion. Newborn CF ferrets mimic meconium ileus (MI) pathology at similar rates to human infants with CF, and newborn CF ferrets show pancreatic disease like humans. Adult CF ferrets also present with a defective exocrine pancreas and malnutrition issues. (27)

Microphysiological systems (MPS), also known as organ-on-a-chip are in vitro platforms that simulate the biochemical and mechanical properties of organs or tissues. MPS allows the study of pathophysiology states, to evaluate xenobiotic toxicities, and the development new therapies. (28) Previous investigations have shown that three-dimensional (3D) MPS can exhibit cell response more comparable to in vivo performance. Cell polarization, for instance, is not steadily maintained in 2D culture of proximal tubule epithelial cells, opposed to what is observed in MPS. (29)

The proximal tubule has been by far the most common segment of the nephron employed in MPS technology. Studies have successfully created devices seeded with proximal tubule epithelial cells capable of recapitulating renal structure and function of the human proximal tubule, such as primary cilium formation, alkaline phosphatase activity, albumin transport, glucose reabsorption, and metabolic and transporter functions. (30) The application of this system allows investigations into compound-specific kidney injury due to the ability of MPSs to mimic physiological function on reabsorption, metabolism, and secretion. The MPS developed by Nortis Bio (See **Figure 2**) has a cell culture format that mimics a renal tubular environment in which the renal proximal tubular epithelial cells (PTEC) adhere to the wall of a 120 μm wide cylindrical channel that traverses a collagen-filled compartment. Under flow provided by a syringe or pneumatic pumps, the PTECs polarize and retain many of its phenotypic characteristics. The Nortis Bio kidney chip system proved to be robust and reproducible by National Center for Advancing Translational Sciences (NCATS) MPS testing laboratories (Texas Agricultural and Mechanical, and Massachusetts Institute of Technology) (30,31).

2. HYPOTHESIS

We hypothesize that loss of CFTR disrupts kidney tubule endocytic function.

Aim 1: Isolation, propagation, and characterization of fPTEC in 2D culture.

Aim 2: Development and optimization of a CF MPS model.

Aim 3: Quantification of albumin uptake in 2D and cubilin shedding in CF MPS effluents.

3. MATERIAL AND METHODS

3.1 Isolation of ferret proximal tubule epithelial cells (fPTEC)

fPTEC were obtained from ferret kidney necropsies in the laboratory of Dr. John Engelhardt (University of Iowa), who developed the original *CFTR* gene edited ferret model and, more recently, has used CRISPR/Cas-9 gene editing to generate a ferret harboring a G551D and ΔF508 *CFTR* mutations.(32) The ferret kidneys were transported under refrigerated conditions in Dulbecco's Modified Eagle Medium: Nutrient Mixture F-12 (DMEM/F12) (Gibco, Waltham, MA) containing 1% of penicillin-streptomycin (Gibco, Waltham, MA) and processed for isolation of proximal tubule epithelial cells within 24 h.

Ferret kidneys were decapsulated under aseptic conditions and perfused with cold DMEM/F12 (Gibco, Waltham, MA) with 1% of penicillin-streptomycin (Gibco, Waltham, MA), 1% of insulin-transferrin-selenium (ITS) (Sigma-Aldrich, St. Louis, MO) and 0.1% of hydrocortisone (Sigma-Aldrich, St. Louis, MO). Cortex was dissected from the medulla using a sterile scalpel. fPTECs were isolated accordingly to previously described procedures (30) with some modification.

The cortex tissue was finely minced on a sterile Petri dish on ice using a pair of sterile razor blades and transferred to a 50 mL falcon tube with a Dulbecco's phosphate-buffered saline solution (dPBS++) (Gibco, Waltham, MA) containing 0.75 mg/mL of collagenase Type IV (Gibco, Waltham, MA) and 0.75 mg/mL of dispase (Gibco, Waltham, MA). The solution was

placed in a 37°C water bath for 10 min followed by incubation for 40 min at 37°C in shaker at 200-220 rpm.

Next, the fragments were vortexed and after sedimentation, the supernatant was collected into a 50 mL falcon tube containing 10 mL of horse serum (Gibco, Waltham, MA) and spun at 200 g for 6 min. The supernatant was aspirated, and the pellet was resuspended in cell media culture, and filtered in a 100 μm pore size strainer to a new 50 mL falcon tube. The process was repeated to wash the cells and the pellet was resuspended and plated into a T75 cell culture flask. Approximately 3 cm^3 of tissue was enough to plate a T75 flask. Media was changed 24 h later and every 48 h until confluency. (30) Cells were incubated in humidified 95% air / 5% CO_2 at 37°C. Following isolation, fPTECs were expanded in tissue culture flasks to passages 1 and 2 before all experiments.

3.2 2D fPTECs culture

The cells isolated were labeled by letters and numbers. Cells isolated from the kidney of wild type ferret were referred as WT, those isolated from a G551D received the nomenclature of M(G551D)# and cells from a ΔF508 ferret were named as ΔF508#. The numbers following the initial description represent the incoming order of kidney received.

fPTEC passages were evaluated on WT2, ΔF508#1 and M(G551D)#5. The cells were plated in a T25 flask in DMEM/F12 (Gibco, Waltham MA) cell culture media supplemented with 1% of penicillin-streptomycin (Gibco, Waltham, MA), 1% ITS (Sigma-Aldrich, St. Louis, MO) and 0.1% of hydrocortisone (Sigma-Aldrich, St. Louis, MO). The cells were grown for 5 days, and microscopy images were acquired at 24 h, 3 days and 5 days after plating. On the sixth

day, cells were trypsinized with 2 mL of trypsin-ethylenediaminetetraacetic acid (EDTA) 0.05% (Gibco, Waltham, MA), resuspended in cell culture media, plated in new T25 flasks and the microscopy images were done at 24 h, 3 days and 5 days later.

The cell culture media optimization was performed on WT2 and M(G551D)#4 in a 24 well plate and we tested DMEM/F12 with 30 mg/dL of glucose (Gibco, Waltham MA) supplemented with 1% of penicillin-streptomycin (Gibco, Waltham, MA), 1% ITS (Sigma-Aldrich, St. Louis, MO) and 0.1% of hydrocortisone (Sigma-Aldrich, St. Louis, MO), DMEM/F12 with 10 mg/dL of glucose (Gibco, Waltham MA) with 1% of penicillin-streptomycin (Gibco, Waltham, MA), 1% ITS (Sigma-Aldrich, St. Louis, MO) and 0.1% of hydrocortisone (Sigma-Aldrich, St. Louis, MO), and DMEM/F12 with 10 mg/dL of glucose (Gibco, Waltham MA) with 1% of penicillin-streptomycin (Gibco, Waltham, MA), 1% ITS (Sigma-Aldrich, St. Louis, MO), 0.1% of hydrocortisone (Sigma-Aldrich, St. Louis, MO) and 0.5% Fetal Bovine Serum (FBS) (Gibco, Waltham, MA). The cells were grown for 8 days, and microscopy images were taken at 24 h, 5 days and 8 days after plating.

3.3 Development and optimization of the CF MPS model

We used the triple single channel platform developed by Nortis Bio (Woodinville, WA). The triple single channel devices were filled with 6 mg/mL rat tail collagen type I (Corning, Tewskbury, MA) and left overnight at room temperature to allow collagen I matrix polymerization. The microfibers inserts were removed from the devices, and the MPS were perfused with DMEM/F12 media for 24 h at 1 μL/min flow rate. The channels were coated with 2.5 μL of 5 μg/mL mouse collagen type IV (BD Biosciences, Bedford, MA) and allowed to rest

for 30 min at 37 °C followed by 1 h perfusion with DMEM/F12 with 10 mg/dL of glucose (Gibco, Waltham MA) with 1% of penicillin-streptomycin (Gibco, Waltham, MA), 1% ITS (Sigma-Aldrich, St. Louis, MO), 0.1% of hydrocortisone (Sigma-Aldrich, St. Louis, MO) and 0.5% FBS at 1 μL/min. (33)

The cell culture of fPTECs were trypsinized and resuspended with DMEM/F12 with 10 mg/dL of glucose (Gibco, Waltham MA) with 1% of penicillin-streptomycin (Gibco, Waltham, MA), 1% ITS (Sigma-Aldrich, St. Louis, MO), 0.1% of hydrocortisone (Sigma-Aldrich, St. Louis, MO) and 0.5% FBS at a concentration of 18×10^6 cells/mL and 2.5 μL was injected into each collagen IV-coated channel of the MPS. Cells were allowed to attach for 10 min before starting flow at a rate of 1 μL/min. (30)

In the optimization experiment, we supplemented the collagen type I matrix with 200 μM of genipin (Fujifilm Wako Chemicals, Richmond, VA) and we tested the collagen I from Ibidi (Madson, WI), in addition to the collagen I from Corning (Tewskbury, MA). We also tested DMEM/F12 with 10 mg/dL of glucose (Gibco, Waltham MA) with 1% of penicillin-streptomycin (Gibco, Waltham, MA), 1% ITS (Sigma-Aldrich, St. Louis, MO), 0.1% of hydrocortisone (Sigma-Aldrich, St. Louis, MO) supplemented with 1 and 2% of FBS and we tested the renal epithelial cell growth medium (REGM) (Lonza, Hayward, CA) supplemented with SingleQuot kit (0.1% insulin, 0.1% hydrocortisone, 0.1% gentamycin, 0.1% transferrin, 0.1% triiodothyronine, 0.1% epinephrin, 0.1% growth hormone (hEGF), and 0.5% FBS) (Lonza, Hayward, CA).The conditions described before were tested in triplicate.

3.4 Immunocytochemistry

fPTECs WT2, ΔF508#1 and M(G551D)#4 and one human PTEC AGJZ-30 were plated in a 8 well slide chamber (Thermo-Fisher, Waltham, MA). After 5 days in 2D culture in the 8 well slide chamber, the cells were fixed with a 4% formaldehyde (Fisher Scientific, Pittsburg, PA) solution at room temperature for 10 min. Permeabilization was performed with 0.1% Triton X-100 (Sigma-Aldrich, St. Louis, MO) for 10 min for the primary antibody zonula occludens 1 (Z01) (Abcam, Cambridge, MA) and for 5 min for the other primary antibodies: CFTR (Abcam, Cambridge, MA); aquaporin 1 (AQP1) (Abcam, Cambridge, MA); aquaporin 2 (AQP2) (Abcam, Cambridge, MA); sodium-glucose co-transporter 2 (SGLT2) (Abcam, Cambridge, MA); epithelial cell adhesion molecule (EpCAM) (Abcam, Cambridge, MA), and epithelial cadherin (E-Cadherin) (Abcam, Cambridge, MA).

Blocking was carried out with 2.5% bovine serum albumin (BSA) (Sigma-Aldrich, St. Louis, MO), and 0.1% Triton X-100 (Sigma-Aldrich, St. Louis, MO) for 1 h. Primary antibodies were applied overnight at 4 °C and fluorescently-labeled secondary antibodies: donkey anti-mouse Alexa-fluor 488 (Abcam, Cambridge, MA), anti-rabbit Alexa-fluor 488 (Abcam, Cambridge, MA), anti-mouse Alexa-fluor 594 (Abcam, Cambridge, MA), and anti-rabbit Alexa-fluor 594 (Abcam, Cambridge, MA) were applied for 1 h at room temperature. Cells were mounted using SlowFade Gold Antifade Mountant (Invitrogen, Carlsbad, CA).

3D fPTEC MPS were grown for 5 days and fixed with a 4% formaldehyde solution at room temperature for 20 min at 6 μL/min flow rate in DMEM/F12 with 10 mg/dL of glucose (Gibco, Waltham, MA) with 1% of penicillin-streptomycin (Gibco, Waltham, MA), 1% ITS

(Sigma-Aldrich, St. Louis, MO), 0.1% of hydrocortisone (Sigma-Aldrich, St. Louis, MO) and 0.5% FBS. Permeabilization was done with a dPBS++ solution containing 0.2% Triton X-100, perfused for 1 h at 6 μL/min at room temperature, and blocking was done with 2.5% bovine serum albumin for 1 h at 4 °C. Primary antibodies Z01 (Abcam, Cambridge, MA), CFTR (Abcam, Cambridge, MA), AQP1 (Abcam, Cambridge, MA), AQP2 (Abcam, Cambridge, MA), SGLT2 (Abcam, Cambridge, MA), EpCAM (Abcam, Cambridge, MA), E-Cadherin (Abcam, Cambridge, MA) , megalin (Abcam, Cambridge, MA), and Na/k ATPase (Abcam, Cambridge, MA) were perfused in the chips for 30 min at 6 μL/min then valves were closed and the antibodies were incubated in the chips overnight at 4 °C. Secondary antibodies donkey anti-mouse Alexa-fluor 488 (Abcam, Cambridge, MA), anti-rabbit Alexa-fluor 488 (Abcam, Cambridge, MA), anti-mouse Alexa-fluor 594 (Abcam, Cambridge, MA), anti-rabbit Alexa-fluor 594 (Abcam, Cambridge, MA), were incubated in the chips for 2 h at room temperature. The primary antibodies were diluted 1:100 and the secondary antibodies were diluted 1:1000 in dPBS++ with 2.5% BSA (Sigma-Aldrich, St. Louis, MO). After that, the chips were washed with dPBS++ solution containing 0.2% Triton X-100 for 2 h before the nuclei staining by perfusion of 1 ug/mL Hoechst 33342 (Thermo-Fisher, Waltham, MA) in dPBS++ for 30 min followed by a 30 min of dPBS++ wash. The cells were imaged on a Nikon Eclipse Ti-S microscope (Melville, NY) equipped with a Nikon DS-Fi3 camera (Melville, NY).

All the primary antibodies applied were human and they were selected based on a previous amino acid sequencing alignment performed using the online tool Clustal Omega (EMBL-EBI) that allows to compare the epitope sequence of each antibody with the ferret amino

acid sequence for each protein of interest to increase the chance of cross-reaction. This step was necessary because so far there is an absence of primary antibodies specific for ferrets.

3.5 Live/Dead staining in fPTEC MPS

We applied a viability kit and Hoechst 33342 to assess the cell viability according to manufacturer's specifications (Life Technologies, Rockville, MD). Calcein AM, Ethidium Homodimer-1 (EthD-1), and Hoechst 33342 were diluted in prewarmed dPBS++ (Gibco, Waltham, MA). fPTEC MPS chips were perfused at 5 μL/min via the luminal port for 20 min at room temperature and after that, MPS chips were transferred into the incubator and remained there for 10 min at 37 °C. After the staining procedure, chips were imaged using fluorescent microscopy. (33)

3.6 Isolation of mRNA and RNA sequencing

We performed RNA sequencing in 3 fPTEC wild types (WT2, WT3 and WT4), 3 fPTEC G551D (M(G551D)#4, M(G551D)#5 and M(G551D)#6) and 1 fPTEC ΔF508 (ΔF508#1), and we had 3 human PTECs samples as control (AGJZ-30, BIO 140 and BIO 142). All samples were 2D cell culture passage 1. fPTEC were harvested from T25 flask using 1 mL of RLT buffer (Qiagen, Valencia, CA). Cell lysates were kept at -80°C until isolation. RNA was isolated using a RNeasy Micro Kit (Qiagen, Valencia, CA) and the RNA library was prepared using Clontech SMARTer Stranded Total RNA Sample Prep Kit (Takara Bio Mountain View, CA). RNA sequencing was performed at 300 cycles in 2 lanes using the Illumina NextSeq 500 High Output v2 Kit. (34,35)

3.7 2-NBD-glucose uptake

Glucose reabsorption via SGLT2 was tested in fPTEC 2D culture and human PTEC were used as control. fPTEC and human PTEC were seeded in a 96 well black plate with a clear bottom at a density of 5 x 10^4 cells/well and grown overnight in DMEM/F12 media. On the next day, cells were treated with vehicle control or 0.5 μM of dapagliflozin (Toronto Research Chemicals, Toronto, ON), a selective SGLT2 inhibitor, in 100 μL of DMEM/F12 with 10 mg/dL of glucose (Gibco, Waltham MA) with 1% of penicillin-streptomycin (Gibco, Waltham, MA), 1% ITS (Sigma-Aldrich, St. Louis, MO), 0.1% of hydrocortisone (Sigma-Aldrich, St. Louis, MO) for 12 h. Cells were treated with 100 μL of 2-NBD-glucose (Thermo-Fisher, Waltham, MA), a fluorescent glucose analog, in DMEM/F12 with 10 mg/dL of glucose (Gibco, Waltham MA) with 1% of penicillin-streptomycin (Gibco, Waltham, MA), 1% ITS (Sigma-Aldrich, St. Louis, MO), 0.1% of hydrocortisone (Sigma-Aldrich, St. Louis, MO) at a final concentration of 0.6 mM and incubated at 37 ℃ for 1 h. After that, the cells were washed three times with dPBS++ and they were imaged using fluorescent microscopy. Biological samples triplicate were analyzed in technical triplicate. Fluorescent signal was quantified using ImageJ software (National Institutes of Health, Bethesda, MD). (30)

3.7 Cubilin ELISA

We performed a multiple sequence alignment using the Clustal Omega program (EMBL-EBI) to select a cubilin antibody that could potentially cross-react with cubilin expressed in ferrets. We selected a human cubilin ELISA from Biomatik (Wilmington, DE) and the experiment was conducted according to the supplier`s guidelines. Effluents from the ferret MPS

bearing the cells, WT1, WT2, ΔF508#3 and ΔF508#4, all passage 2, were collected 96 h after the cell seeding. We applied 100 μL of effluents to the assay and each sample was analyzed by technical triplicates. The samples were analyzed in a microplate reader (Tecan Spark, Redwood, CA). The levels of cubilin in the effluents were below the limit of detection.

3.8 2D Albumin uptake

The albumin uptake was performed in 2D with the fPTEC WT2, and ΔF508#1. The human PTEC AGJZ-30 was included as control. The cells were plated in 96 well black plate with a clear bottom at a density of 5 x 10^4 cells/well and grown overnight in DMEM/F12 with 10 mg/dL of glucose (Gibco, Waltham MA) with 1% of penicillin-streptomycin (Gibco, Waltham, MA), 1% ITS (Sigma-Aldrich, St. Louis, MO) and 0.1% of hydrocortisone (Sigma-Aldrich, St. Louis, MO). On the next day, cells were incubated for 30 min with 50 μg/mL albumin-FTIC (Abcam, Cambridge, MA) or albumin-FTIC and 1 μM receptor-associated protein (RAP) (Innovative Research, Novi, MI) endocytic inhibitor as described previously. (36) After the incubation, the cells were washed 3 times with cold dPBS++ and then lysed with 200 μL of 0.5% Tween 20 (Sigma-Aldrich, St. Louis, MO) in dPBS++. The lysate was analyzed in fluorescence plate reader (Tecan Spark, Redwood, CA). Biological samples triplicate was analyzed in technical triplicate. The levels of albumin-FITC were below the limit of detection.

3.9 Data Analysis

The comparations performed between fPTEC and human PTEC regarding the RNA transcripts for EMT markers was performed by fold change. For the comparison of means in the

2-NBG glucose uptake experiment, statistical test (unpaired, Student`s T-test) was applied using GraphPad software (La Jolla, CA). Statistical significance was considered at p values < 0.05.

4. RESULTS AND DISCUSSION

4.1 Isolation and propagation of ferret proximal tubule epithelial cells (fPTECs)

During the development of this project, we isolated the proximal tubule epithelial cells (PTEC) of 6 wild type, 11 G551D, and 4 ΔF508 ferret kidneys. As described in material and methods, WT refers to the cells isolated from a wild type kidney, M(G551D)# indicates the cells isolated from a G551D kidney and ΔF508# the cells isolated from a ΔF508 kidney. All the labels were followed by numbers as a sequence of the kidneys received.

We observed the formation of small colonies 24 h after the cell isolation. Confluent monolayers with a cobblestone-like appearance, typical of epithelial cells, were formed in approximately 7 days, (See **Figure 3**) while domes, also called hemicysts, were produced in the cell culture on day 10 (See **Figure 4**). Hemicysts are characteristic of PTEC, and results from fluid transport below the cell monolayer, elevating the culture surface. (37) The morphological development of the primary cells isolated from wild and CF ferrets agreed with previous studies on human and mouse PTEC. (30,38–40)

fPTECs kept cobblestone-like appearance for at least 3 days for passages 1 and 2 and started transitioning to a mixed population with a cobblestone-like and flat morphology at day 5 while cultured in DMEM/F12 media **(**See **Figure 5)**. The use of DMEM/F12 with low glucose levels (10 mg/dL) supplemented with 0.5% FBS kept the population of cobblestone-like cells more uniform for 8 days at passage 2 on WT2, and M(G551D)#4 **(**See **Figure 6)**. Renal

epithelial cells can undergo epithelial mesenchymal transition (EMT) during renal injury and at high glucose levels. (41,42)

The reduction in glucose concentrations of the media from 30 to 10 mg/dL, and the supplementation with hormones, lipids, and growth factors from FBS might have contributed for the prevalence of a cobblestone-like cells morphology for 8 days suggesting that media modification stimulated the growth of epithelial cells while reducing the formation of cell with the flat morphology.

4.2 Development and optimization of the CF MPS model

The aim 2 of this work was to develop and optimize the CF MPS model. For that, fPTECs were injected into the MPS and approximately 10 min later, we observed through microscopy the cell adhesion to the inner surface of the channel. The fPTEC adhesion was faster than human PTEC which takes around 3 h to occur. (30) Between 48 and 72 h after the injection, we observed the migration of flat and elongated cells out of the channel, invading the collagen matrix, **(**See **Figure 7)** and clumping within the lumen.

In order to improve the channel formation, we introduced 200 μM genipin in collagen I to reduce cell migration. Genipin has been employed as a cross-linking agent to prevent cell migration. (43) Addition of genipin restricted the cell movement out of the tubules. We also tested different concentrations of FBS (1 or 2%) to improve the growth and division of epithelial cells, while minimizing the acquisition of cell with flat morphology and cellular clumping. No change was observed in cellular morphology with FBS.

We also investigated different brands of collagen I used in the preparation of the MPS tubules. The Ibidi collagen type I provided tubes that decreased the fPTEC clumping, but it was ineffective in inhibiting changes in cell morphology (See **Figure 8).** The reduced levels of cell agglutination might be explained by the lower amount of acetic acid in the Ibidi collagen type I compared to Corning (17.5 mM vs. 20.0 mM). fPTEC may be more sensitive to pH variation than human PTEC. Additional experiments are needed to better understand these results.

We examined whether replacing the culture medium with renal epithelial cell basal medium (REGM) could help to preserve the cell morphology and to decrease the cell migration. REGM has been used in renal primary rodent culture and promotes the epithelial cell morphology. (40,44) In our studies, REGM with supplements, reduced cell clumping and the presence of flat and elongated cells (See **Figure 9**). Although the nutritional composition of REGM is not disclaimed, we can infer some of the effects of the known compounds in the medium. Epinephrine, triiodothyronine, and hEGF can induce cell proliferation and differentiation; (45–47) however, there is no information concerning their effect on cell clumping.

4.3 fPTEC characterization in 2D and in MPS

To characterize the proximal tubule and epithelial origin of the cells, we applied immunocytochemistry and RNA sequencing techniques. RNA sequencing can provide a snapshot of the RNA transcripts; however, it cannot point to the presence of a protein; for this reason, this method is coupled to immunocytochemistry that can confirm the occurrence of a protein of interest.

Principal component analysis (PCA) of the RNA transcripts was used to answer the question whether the RNA expression differs among the fPTEC genotypes; however, the PCA analysis did not indicate a distinct pattern of expression between wild types and the *CFTR* variants G551D and ΔF508 (See **Figure 10**). We examined the RNA expression of proximal tubule markers angiotensinogen (AGT) and AQP1 and distal tubule markers AQP2 and prominin-2. (30,48) WT2, WT4 and M(G551D) #6 were expressing AGT whereas AQP1 was expressed just in ΔF508#1. AQP2 and prominin 2 were not expressed in any samples (See **Figure 11**). The absence of RNA expression for AQP1 may indicate that the cells were not expressing that protein at the moment that cells were harvested since immunocytochemistry confirmed the presence of AQP1 protein. The absence of AQP2 protein was also confirmed through immunocytochemistry.

In terms of epithelial markers, we noticed the RNA expression of ZO1 in WT3, WT4, M(G551D)#4, M(G551D)#6, and ΔF508#1 which was confirmed by immunocytochemistry. (See **Figure 11 and 12**). Although CFTR was absent in RNA sequencing, the protein presence was confirmed in immunocytochemistry analysis. We did not observe ICC staining for SGLT2 and EpCAM in ferret samples, but we noticed RNA expression for those proteins showing transcription activity in the cells, indicating a possible lack of cross-reactivity for the antibodies applied. We also did not find expression of megalin by RNA sequencing for the ferret and human samples, but we noticed a speckled signal when performing immunocytochemistry on 2D and MPS samples for human (see **Figure 13**). Megalin is an endocytic receptor that can be found in vesicles (19) suggesting a possible staining in endosomes rather than the cell surface of the sample controls.

fPTECs presented approximately 2-fold increase of the EMT markers α smooth muscle actin (αSMA), and fibronectin 1, (49,50) (See **Figure 14**) when compared to human PTECs, suggesting the fPTECs are transforming into a more fibroblast-like morphology. ICC staining for vimentin, αSMA and fibronectin 1 is needed to confirm protein expression in the cell. The expression of vimentin, αSMA and fibronectin 1 could also be a characteristic of fPTECs, but there is no literature to compare the observed data. fPTEC MPS immunocytochemistry was performed in one ferret WT1 passage 2, and one ΔF508#4 passage 1. ICC staining resulted in nonspecific signal for AQP1, ZO1 and CFTR, indicating a necessity for ICC optimization in MPS. We noted specked green signal for megalin indicating possible protein expression (See **Figure 15 and 16**). No stained was obtained for SGLT2, AQP2, EpCAM and Na/k. Cell viability of fPTECs was 100% when cultured in MPS for 5 days as no red staining indicating dead cells was observed (See **Figure 17**).

In addition to the immunocytochemistry and RNA sequencing techniques, we performed functional tests for glucose uptake in the fPTEC in 2D culture. We observed a reduction in the glucose uptake by a reduction in 2-NBD glucose fluorescence in the group receiving 0.5 μM dapagliflozin which is a selective SGLT2 inhibition, indicating the functionality of SGLT2 in the ferret cells (See **Figure 18**).

4.4 Quantification of albumin uptake in 2D and cubilin shedding in fPTEC MPS effluents

In this study, we attempted to answer our hypothesis by evaluating the endocytic function on proximal tubule by analyzing the albumin uptake in the proximal tubule cells and the cubilin shedding on MPS effluents. Under the experimental conditions, no cubilin shedding was detected

by ELISA and we were not able to measure the endocytosis of labeled albumin since the levels of FITC-albumin were below of the limit of detection. The results generated are inconclusive and further optimization of fPTEC MPS development is required to respond whether the absence of CFTR impairs the endocytic function on renal proximal tubule.

4.5 Limitations and future directions

There are some limitations in the development of MPS with fPTECs. There are no commercially available antibody-based reagents specific for ferrets, which impacts protein analysis by either immunocytochemistry or ELISA-based biomarker quantitation. The caveat of using antibodies with uncharacterized specificity can result in weak signal due to lack of cross-reactivity, may not accurately identify the expression and/or subcellular localization of the target antigen in ferret cells, or may have non-specific binding to other proteins that would result in a false-positive signal.

There are a number of issues encountered in trying to generate 3D MPS populated with confluent fPTEC monolayers and one of these issues was cell clumping. Factors involved in cell clumping are over-digestion of tissue and environmental stress resulting in lysis of the cells and release of DNA fragments. (51) From this perspective, including DNase I into the cell isolation process can help to digest DNA. Replacing collagenase with an enzyme more specific for cleaving epithelial tissue such as dispase, decreasing the time of tissue incubation with collagenase during the isolation process and employing a lower rate of flow in the MPS could minimize cell death and the presence of DNA fragments if that were the case. The cell clumping

observed in the fPTECs might have causes inherent to this type of cell yet to be uncover and future advancement can point out other alternatives to mitigate cell clumping in fPTECs.

Another issue we encountered was invasion of the cells into the collagen I matrix. Experiments to address this could include increasing the concentration of type I collagen, the use of varying concentrations of genipin or altering the composition of the media with serum supplementation or defined growth factors as are present in REGM (Lonza, Hayward, CA).

Finally, the presence of mixed population of cells with cobblestone-like morphology and flat morphology in passages 1 and 2 could be the caused by EMT; ICC staining for EMT markers such as α SMA and vimentin could identify if that were the case. Following confirmation, 1 μM of GW788388 hydrate which is a selective TGF β inhibitor can be employed in cell culture media. Previous work has shown that 1 μM GW788388 hydrate was effective in retaining epithelial morphology in iPSC-derived renal proximal tubule cells for at least up to 12 days after passage. In contrast, in the absence of treatment, the cell culture changed morphology to fibroblast-like after 4 days in culture, (52) similar to our results with fPTECs. Another approach would be to co-culture fPTEC with irradiated mouse fibroblasts and Rho kinase inhibitor (Y-27632). This method has been applied to promote cell growth and to prevent spontaneous differentiation. (53–55)

The further development of the fPTEC MPS will allow us to address the hypothesis presented in this work and when fully optimized, the fPTEC MPS can be applied for future modeling the CF kidney function and responses to antibiotic-induced AKI.

5. CONCLUSIONS

In conclusion, we isolated, propagated, and characterized primary epithelial proximal tubule cells from ferret kidneys, and we optimized the cell culture media to minimize transition from epithelial to fibroblast-like morphology in 2D. Furthermore, we created a fPTEC MPS, and we optimized the tubule formation by minimizing cell aggregation and cell transition to a flat morphology in 3D culture. We noticed a functional response to SGLT2 inhibition in 2D culture suggesting that the proximal tubule glucose reabsorption function might not be impaired in cystic fibrosis, but additional analysis will be necessary to confirm that. Additional studies will be needed to respond our hypothesis whether the loss of CFTR disrupts the endocytic function on kidney proximal tubule. Future efforts to improve the fPTEC MPS could focus on incorporating additional supplement to the cells culture and to modify the composition of the collagen I matrix in the MPS.

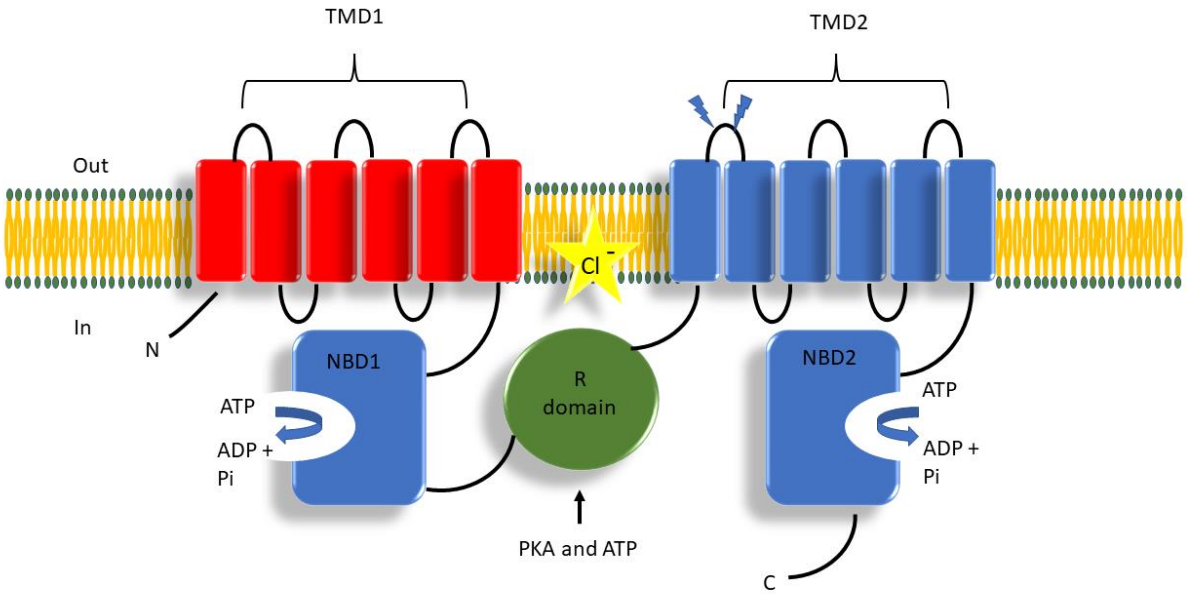

Figure 1. Schematic representation of cystic fibrosis transmembrane regulator (CFTR). Illustration based on reference (56). Nucleotide-binding domain, NBD; regulatory domain, R; transmembrane domain, TMD; protein kinase A, PKA; adenosine triphosphate, ATP; adenosine triphosphate, ADP.

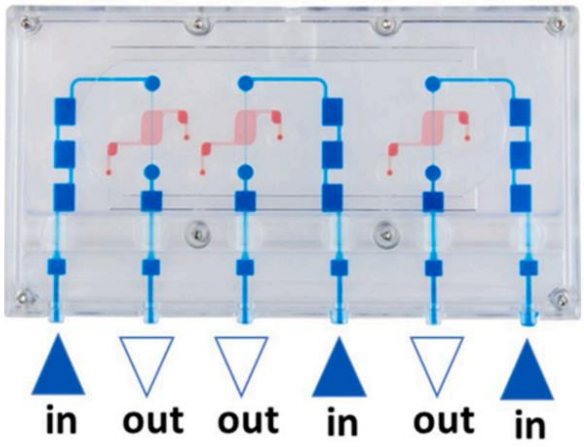

Figure 2. Schematic representation of the microphysiological system (Nortis Bio). The Nortis Bio microfluidic device is composed of a polydimethylsiloxane mold enclosed in a polycarbonate case and microscope coverslip. The mold creates three independent flow paths (blue) through which media is continuously perfused. The pink region indicates the matrix of collagen I which includes the microscope coverslip overlay to facilitate real-time imaging of the MPS tubules within the collagen I matrix.

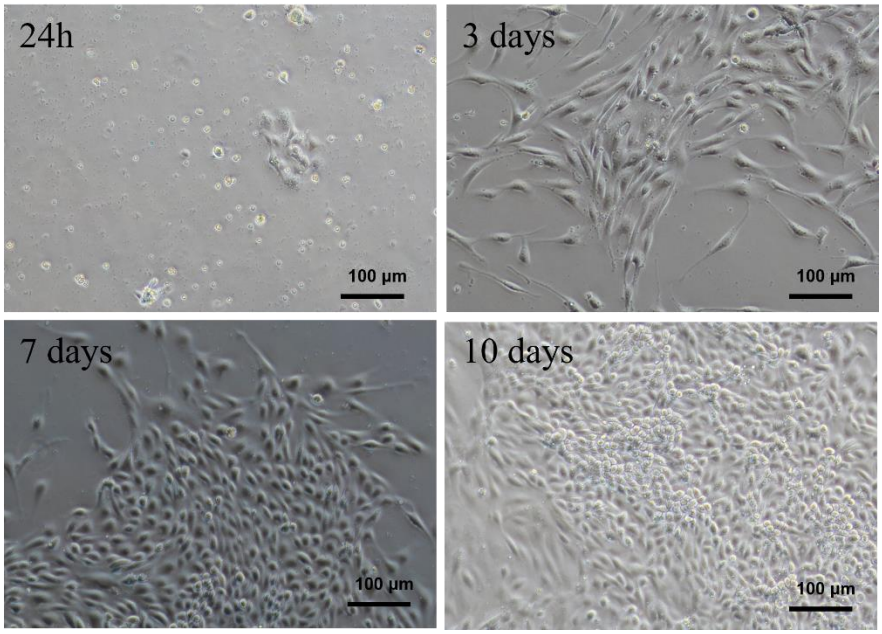

Figure 3. Ferret proximal tubule epithelial cell morphology. Phase contrast microscopy of WT6 (wild type) fPTECs at 24h, 3 days, 7 days, and 10 days after isolation. (Scale bars = 100 µm)

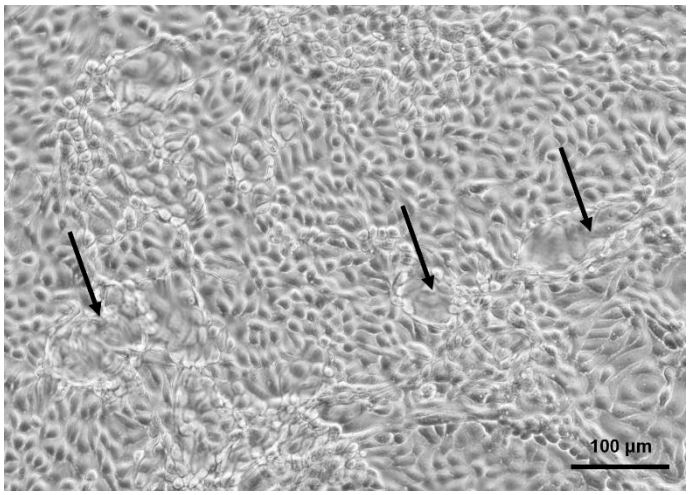

Figure 4. Dome formation in fPTEC. Phase contrast microscopy of fPTECs in 2D culture. The black arrows indicate examples of hemicyst or dome formation as a result of fluid transport. (fPTEC are from donor WT5 at 10 days post isolation). (Scale bar = 100 µm)

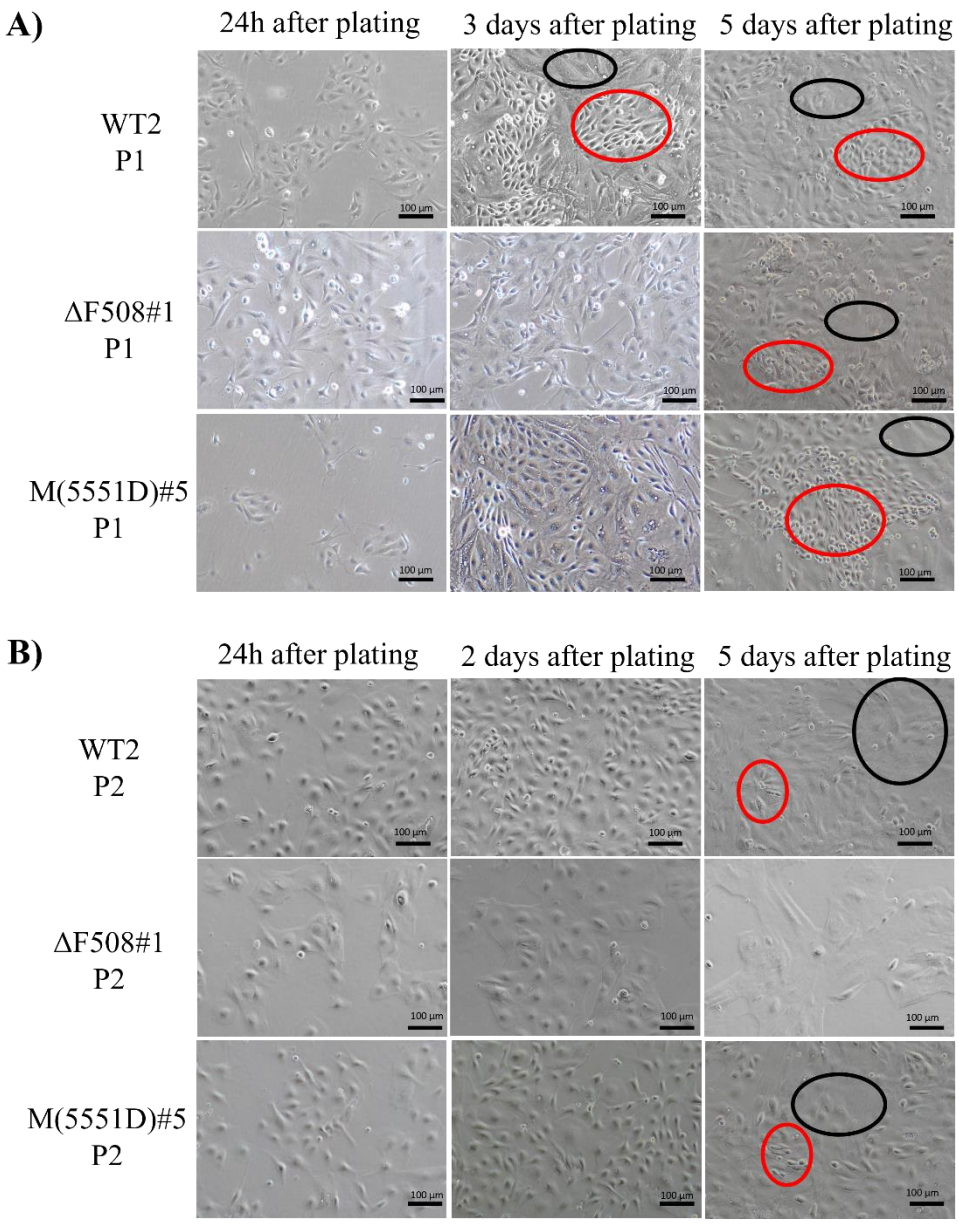

Figure 5. Ferret proximal tubule epithelial cell morphology over passages 1 and 2. Phase contrast microscopy of fPTECs of varying *CFTR* genotypes in 2D culture. **A)** Figure indicates ferret cells morphology 24 h, 3 days and 5 days after plating to passage 1. **B)** Figure represents ferret cell morphology 24 h, 2 days and 5 days after plating in to passage 2. The black circles indicate a population of cells with flat morphology differing from the population confined in the red circles with cobblestone-like morphology. WT2 indicates cell isolated from the second kidney received from a wild type ferret, ΔF508#1 is the label for cell isolated from the first kidney received from a ΔF508 ferret, and M(G551D)#5 refers to cell isolated from the fifth kidney received from a G551D ferret. P1 indicates passage 1 and P2 refers to passage 2. (Scale bars = 100 μm)

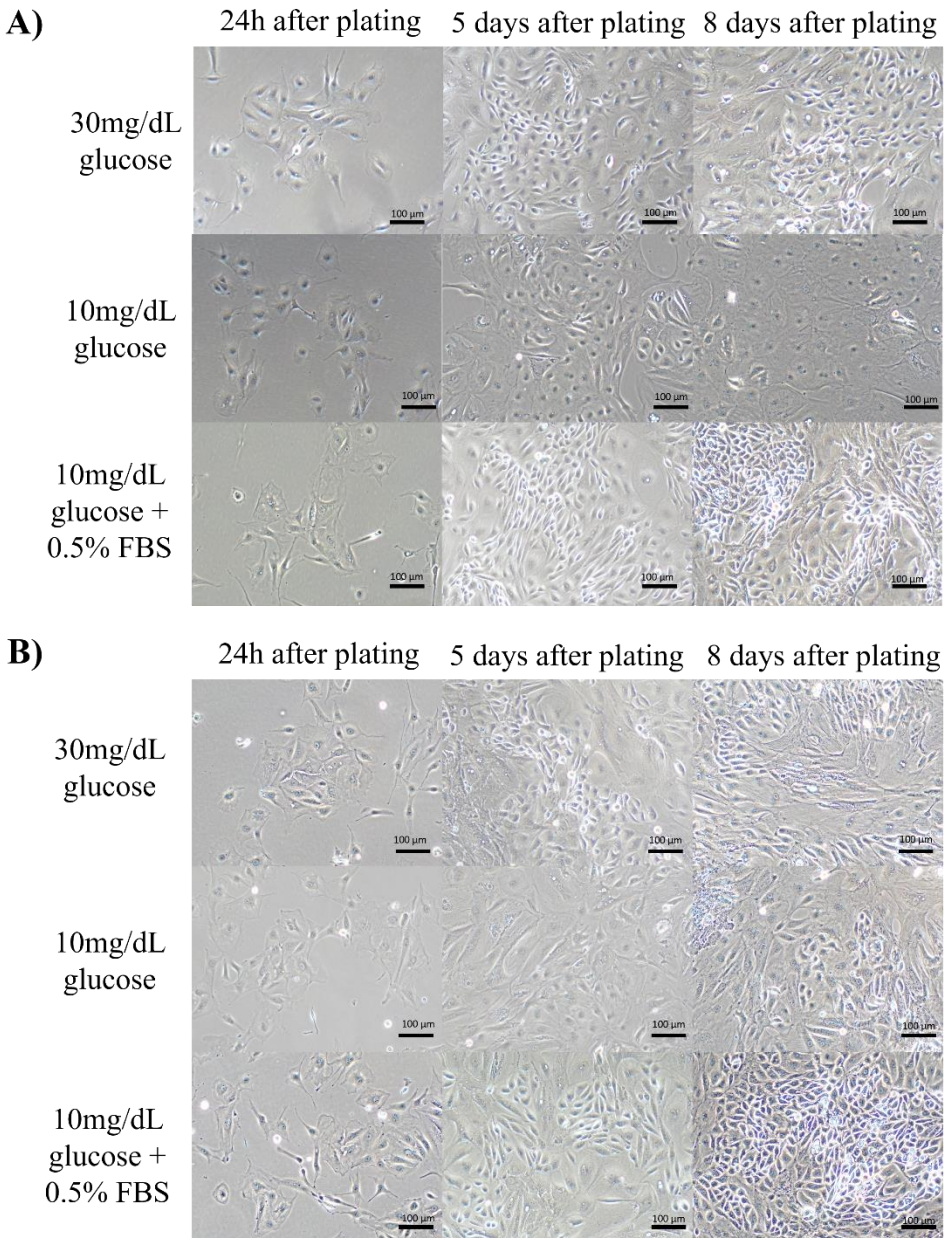

Figure 6. Ferret proximal tubule epithelial cell morphology in cell culture media. Phase contrast microscopy of fPTECs in 2D culture. **A)** Cell morphology of WT2 in DMEM/F12 (30 mg/dL glucose), DMEM/F12 (10 mg/dL glucose), or DMEM/F12 (10 mg/dL glucose) + 0.5% FBS. **B)** Cell morphology of M(G551D)#4 in DMEM/F12 (30 mg/dL glucose), DMEM/F12 (10 mg/dL glucose), or DMEM/F12 (10 mg/dL glucose) + 0.5% FBS. Cell were grown in 24 well plate. WT2 indicates cell isolated from the second kidney received from a wild type ferret, and M(G551D)#4 refers to cell isolated from the fourth kidney received from a G551D ferret. P2 refers to passage 2. (Scale bars = 100 μm)

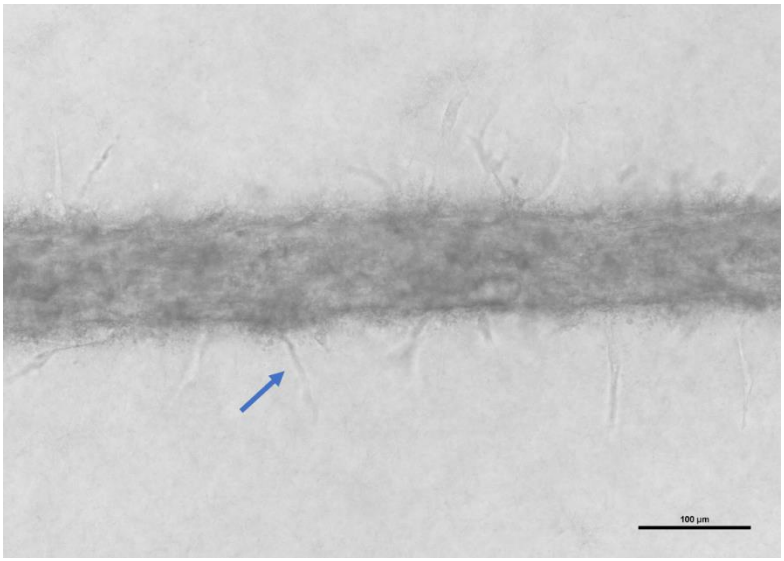

Figure 7. Ferret proximal tubule epithelial cell morphology for WT2 passage 2 inside the MPS. Phase contrast imaging of fPTECs cultured in 3D Nortis Bio MPS culture. The image was acquired 3 days post-injection. Arrow indicates cell protrusions. WT2 indicates cell isolated from the second kidney received from a wild type ferret. MPS: Microphysiological system. (Scale bars = 100 µm)

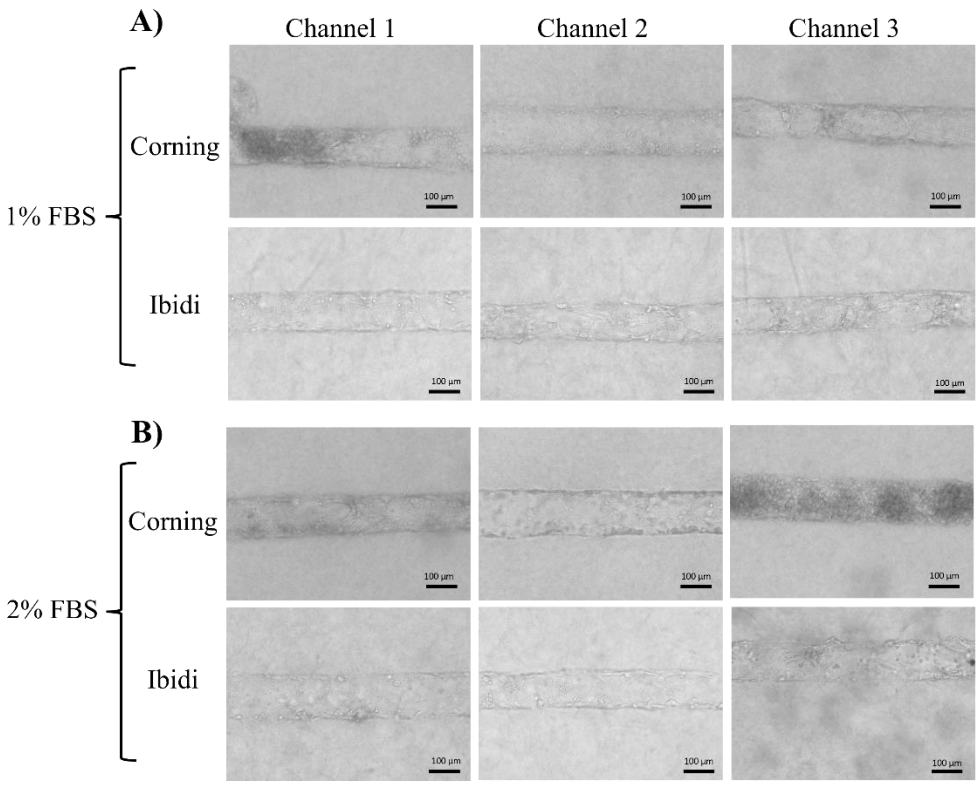

Figure 8. Morphology of the fPTEC WT2 in two commercial sources. Phase contrast imaging of fPTECs cultured in 3D Nortis Bio MPS culture. **A)** Representative images of individual channels of MPS perfused with 1% FBS or **B)** 2% FBS-containing DMEM/F12 media. The top rows in panels A and B are of MPS containing collagen I extracellular matrix purchased from Corning (Tewskbury, MA) while the bottom panel utilized collagen I from Ibidi (Madson, WI). (n=4 MPS per condition tested) (Scale bars = 100 μm)

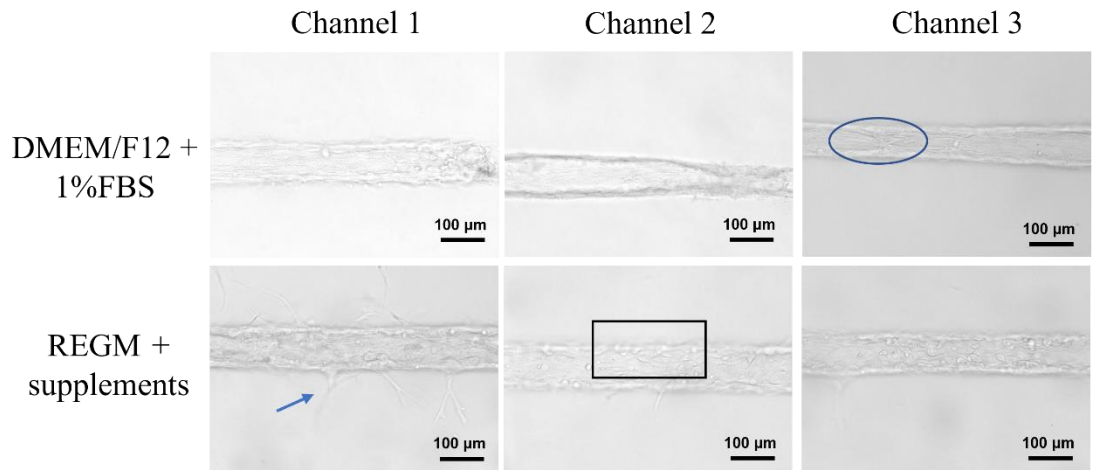

Figure 9. Comparison of media formulations on gross morphology of the fPTEC WT2 3D MPS. Phase contrast imaging of fPTECs cultured in 3D Nortis Bio MPS culture. Top panel depicts three individual channels from an MPS cultured with standard media (DMEM/F12) supplemented with 1% FBS. Bottom panel depicts three individual channels fPTEC grown in REGM media with supplements for 5 days. Picture shows clumping (blue circle) in the fPTEC receiving DMEM/F12 (10 mg/dL glucose) + 1% FBS media. fPTEC treated with REGM with supplements presented cell protrusions in one channel and a cobblestone-like morphology (black square) characteristic of hPTEC (human PTEC). This experiment was conducted with fPTEC from donor (WT2) using cells at passage 2. (n=1 MPS per condition tested) (Scale bars = 100 µm)

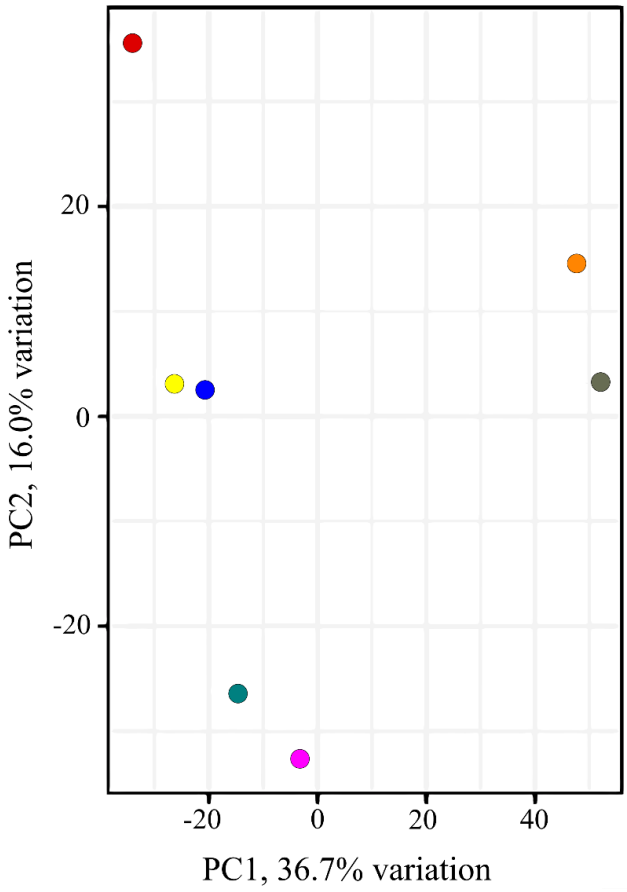

Figure 10. Principal component analysis of the RNA expression in ferret cells in 2D culture at passage 1. No correlation in the RNA expression profile was observed between wild type, G551D and ΔF508 ferrets. WT2 (blue dot), WT3 (pink dot), WT4 (grey dot), M(G551D)#4 (green dot), M(G551D)#5(yellow dot), M(G551D)#6 (orange dot), and ΔF508#1(red dot)

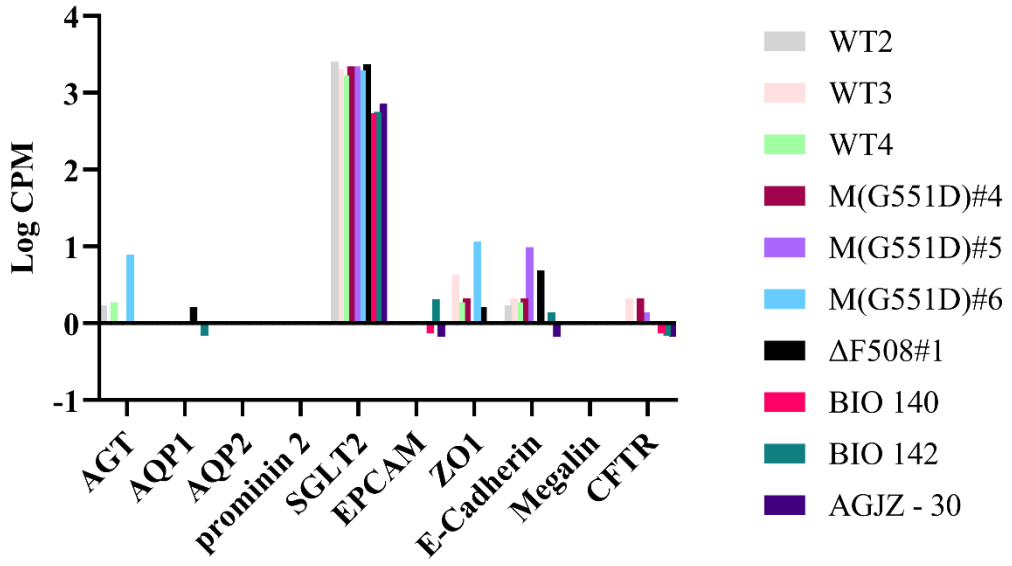

Figure 11. RNA expression of proximal tubule markers (AGT, AQP1), distal tubule markers (AQP2 and prominin 2) epithelial markers (EpCAM, ZO1, E-Cadherin) SGLT2, megalin and CFTR from ferret cells cultivated in 2D. The graph shows the RNA expression for proximal and epithelial markers and the absence of transcripts for distal tubule markers. There is also expression of SGLT2, and absence of expression for megalin in fPTEC. The absence of bars indicates absence of transcription. Results are expressed as log of counts per million (CPM). All cells are passage 1.

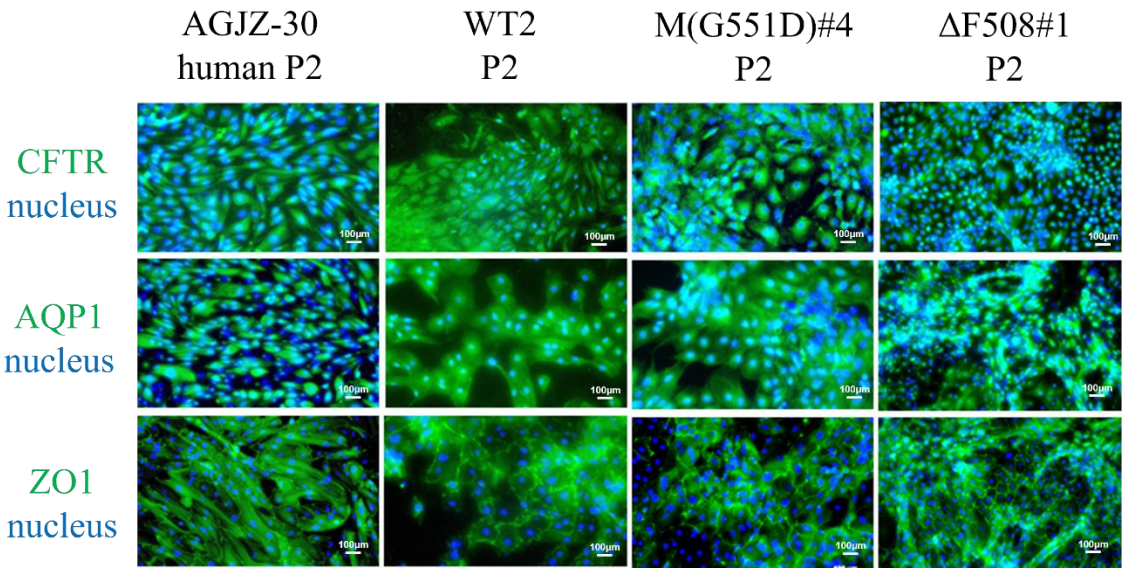

Figure 12. Immunocytochemistry of fPTEC in 2D culture. Cells were cultured, fixed, and stained as described in Material & Methods. In the top panel, cells were assessed for the expression of CFTR, the middle panel for aquaporin 1 (AQP1) and the bottom panel for zona occludens 1 (ZO1). Cells in the first column are from a human PTEC donor and columns 2-4 contain cells from wild type, G551D or Δ508 *CFTR* fPTECs, respectively. All four cell donors tested were from culture passage 2. Nuclei are stained in blue. (Scale bars = 100 μm)

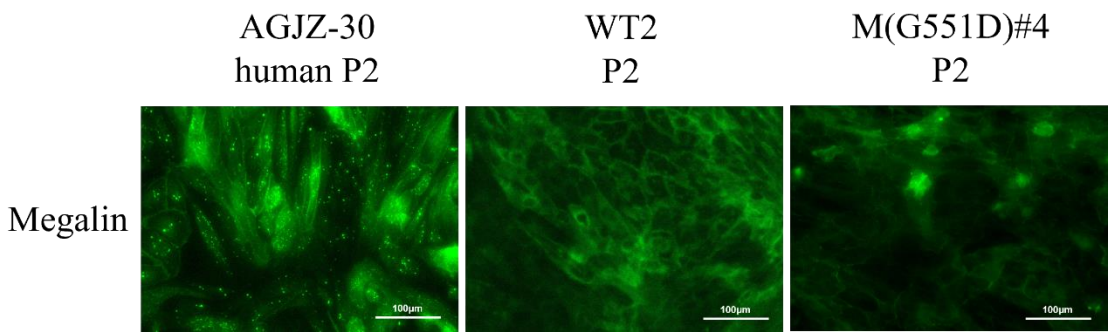

Figure 13. Megalin PTEC expression. Fluorescent imaging of PTECs in 2D culture. Cells were cultured, fixed, and stained for the presence of megalin as described in Material & Methods. In the first panel, cells from a human PTEC donor showed a punctate signal in green that indicates possible expression of megalin in vesicles. In the second panel, WT2 indicates wild type fPTECs, while in the third panel M(G551D)#4 are from a G551D *CFTR* genotype fPTEC. P2 refers to passage 2. (Scale bars = 100 μm)

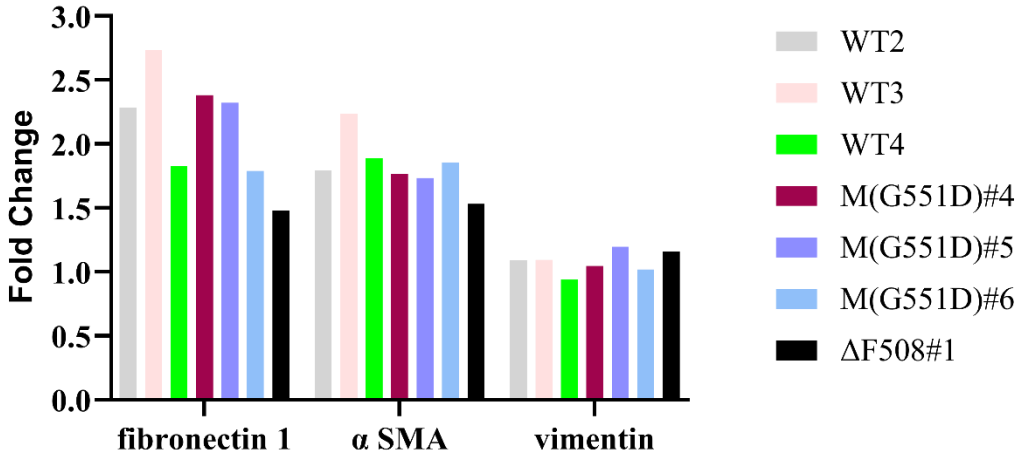

Figure 14. RNA expression for epithelial mesenchymal transition (EMT) markers in fPTEC. Results show approximately 2-fold increase in the expression of EMT markers for fibronectin 1, and αSMA in the fPTEC samples (WT2, WT3, WT4, M(G551D)#4, M(G551D)#5, M(G551D)#6 and ΔF508#1) when compared to the human PTEC samples (BIO 140, BIO 142 and AGJZ-30). All the cells are passage 1.

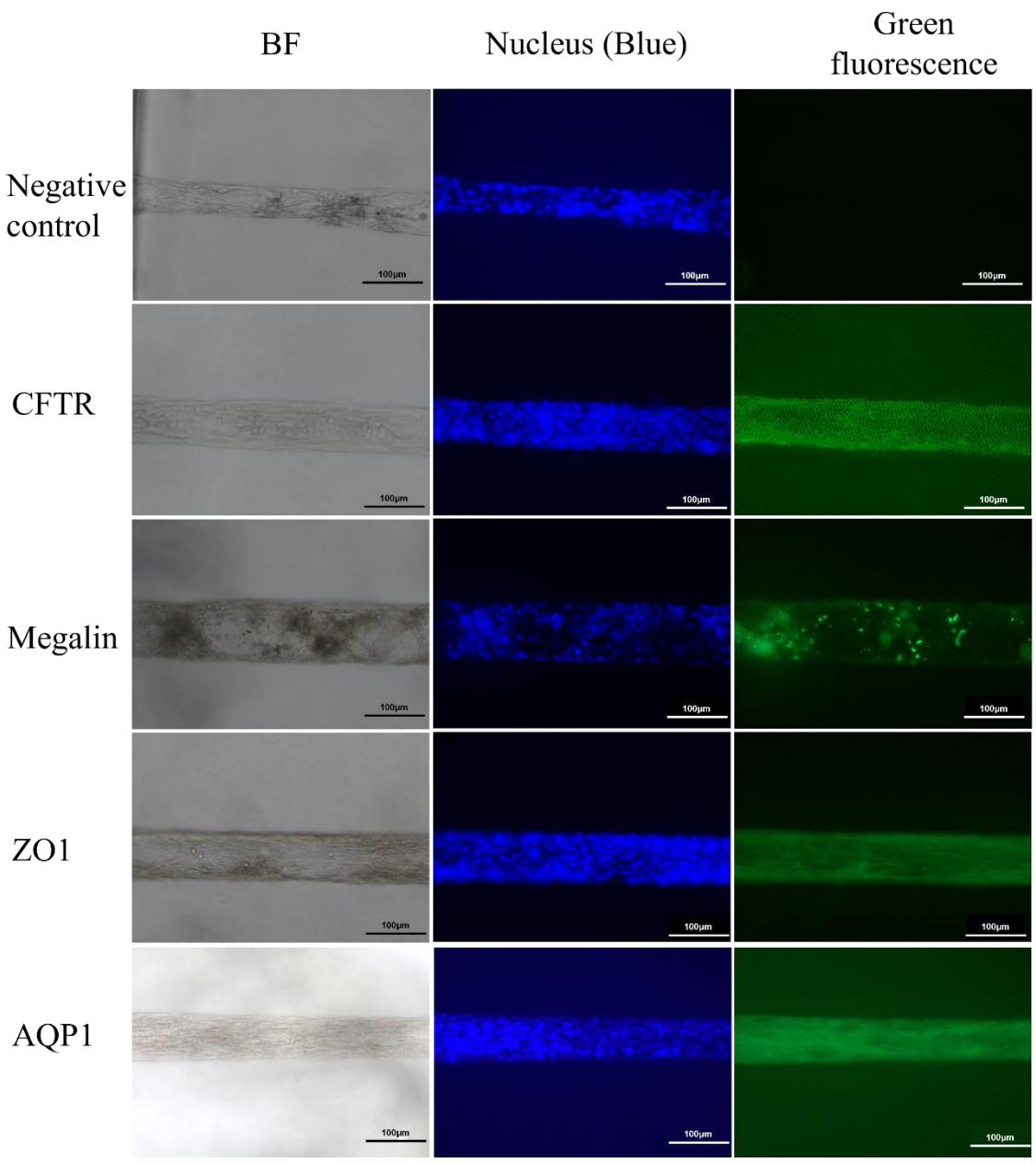

Figure 15. Immunocytochemistry in fPTEC MPS WT1. Each row of the image depicts one channel of the fPTEC MP. The first column of the image indicates a bright field image (BF) of the channels, the second column shown nucleus staining in blue and the third column represents the green fluorescence of the channel. WT1 indicates cell isolated from the first kidney received from a wild type. The cells applied were passage 2. (Scale bars = 100 µm)

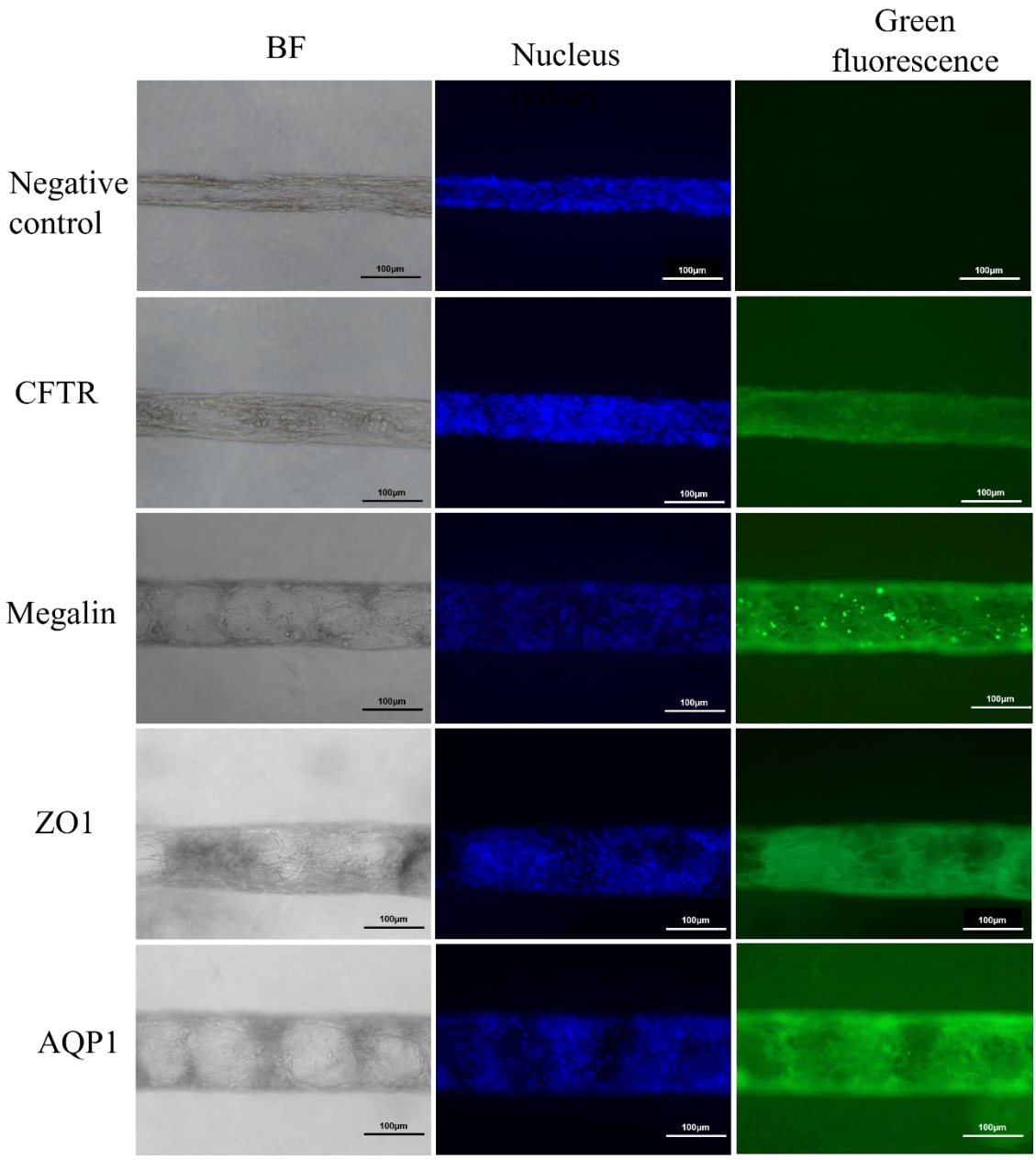

Figure 16. Immunocytochemistry in fPTEC MPS in ΔF508#4. Each row of the image depicts one channel of the fPTEC MP. The first column of the image indicates a bright field image (BF) of the channels, the second column shown nucleus staining in blue and the third column represents the green fluorescence of the channel. ΔF508#4 indicates cell isolated from the fourth kidney received from a ΔF508 *CFTR* genotype. The cells applied were passage 2. (Scale bars = 100 µm)

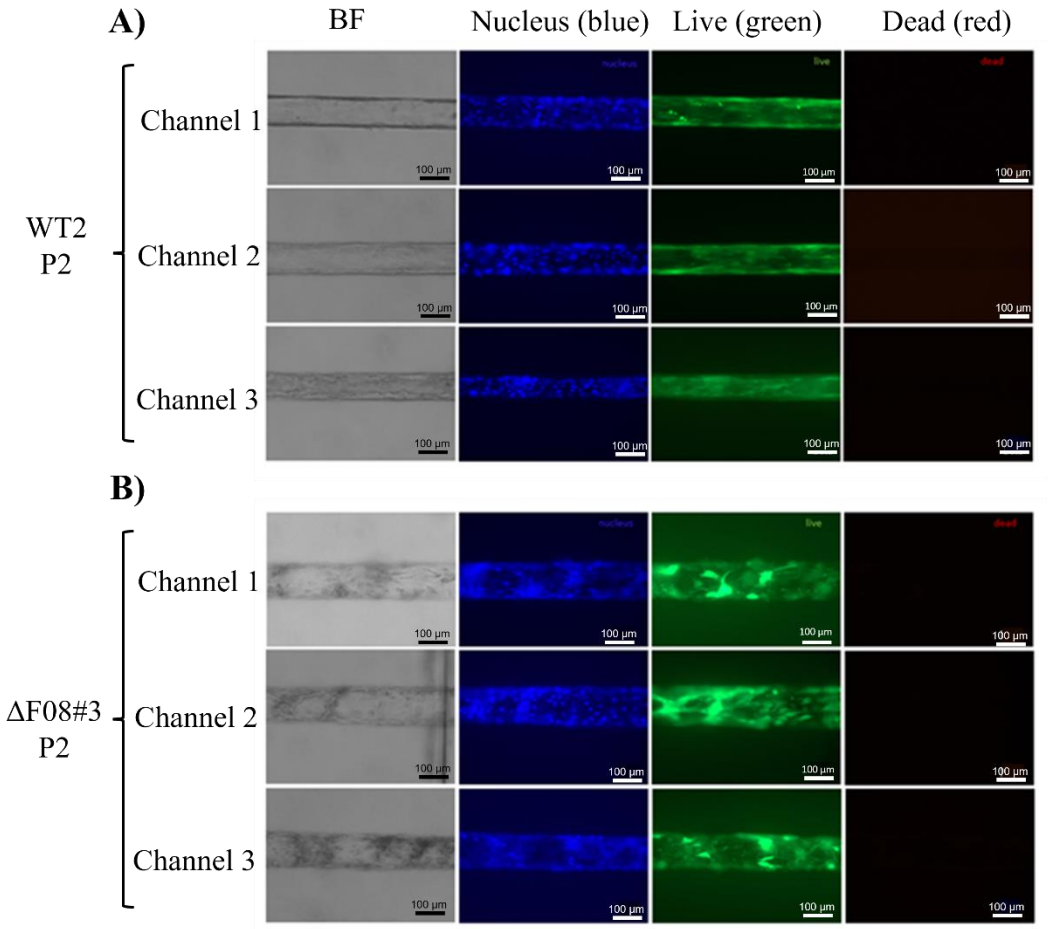

Figure 17. Live/dead staining in fPTEC MPS. Each row of the image depicts one channel of the fPTEC MP. The first column of the image indicates a bright field image (BF) of the channels, the second column shown nucleus staining in blue, the third column represents viable cells in green and the last column detects dead cells in red. **A)** WT2 indicates cell isolated from the second kidney received from a wild type and **B)** ΔF508#3 indicates cell isolated from the third kidney received from a ΔF508 *CFTR* genotype. The cells applied were passage 2. (Scale bars = 100 µm)

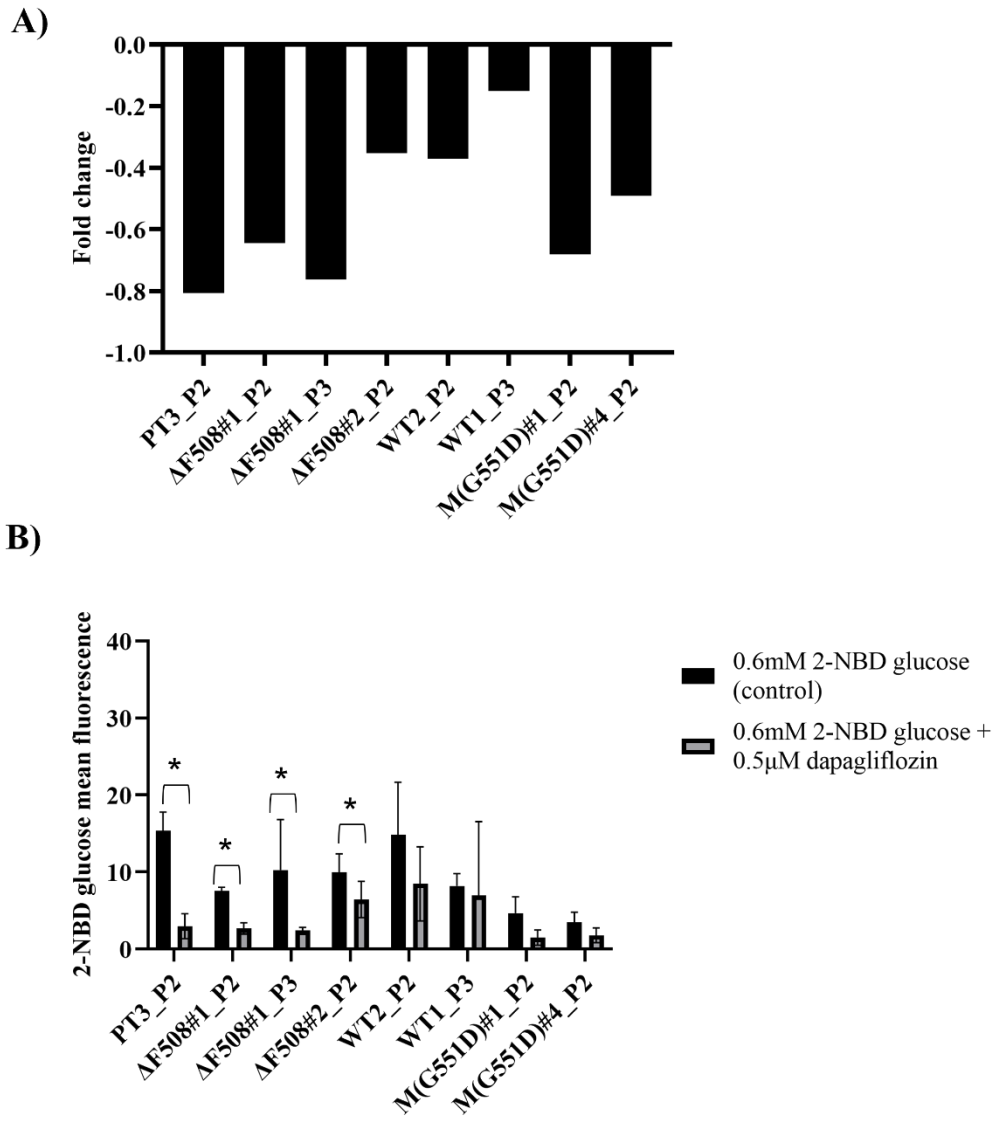

Figure 18. 2NBD-glucose-uptake in 2D fPTEC. A) Quantification of fluorescent signal, demonstrating a fold change reduction in the 2-NBD glucose fluorescence in presence of dapagliflozin in fPTEC. **B)** The ΔF508 fPTECs ΔF508#1 passage 2 (P2), ΔF508#1 passage 3 (P3) and ΔF508#2 passage 2 (P2) showed significant reduction ($p<0.05$, t-test) of glucose uptake in the presence of dapagliflozin. Human PTEC (PT3) was used as positive control. The fPTEC control group was treated with 0.6 mM 2-NBG glucose (fluorescent glucose analog) and the other group received 0.6 mM 2-NBG glucose in the presence of 0.5 μM dapagliflozin (SGLT2 inhibitor). The experiment was conducted in technical and biological triplicates.

6. REFERENCES

1. Scotet V, L'Hostis C, Férec C. The Changing Epidemiology of Cystic Fibrosis: Incidence, Survival and Impact of the CFTR Gene Discovery. Genes (Basel) [Internet]. 2020 May 26;11(6):589. Available from: https://pubmed.ncbi.nlm.nih.gov/32466381

2. Lewis D. Cystic Fibrosis in Primary Care. In: Cystic Fibrosis in Primary Care. First. Switzerland, AG: Springer Nature; 2020. p. 9–25.

3. Steven M. Rowe, M.D., Stacey Miller, B.S., and Eric J. Sorscher M. Cystic fibrosis. Cent Dis Control. 2000;196(5):1–6.

4. Mehta A. CFTR: More than just a chloride channel. Pediatr Pulmonol. 2005;39(4):292–8.

5. O'Sullivan BP, Freedman SD. Cystic fibrosis. Lancet [Internet]. 2009;373(9678):1891–904. Available from: http://dx.doi.org/10.1016/S0140-6736(09)60327-5

6. Keogh RH, Szczesniak R, Taylor-Robinson D, Bilton D. Up-to-date and projected estimates of survival for people with cystic fibrosis using baseline characteristics: A longitudinal study using UK patient registry data. J Cyst Fibros [Internet]. 2018;17(2):218–27. Available from: https://doi.org/10.1016/j.jcf.2017.11.019

7. Cystic Fibrosis Foundation Patient Registry [Internet]. 2017 Annual Data Report. 2018. p. 1–96. Available from: https://www.cff.org/Research/Researcher-Resources/Patient-Registry/2017-Patient-Registry-Annual-Data-Report.pdf

8. Brayshaw S. Cystic Fibrosis: Life Expectancy [Internet]. [cited 2021 Aug 30]. Available from: https://www.nationaljewish.org/conditions/cystic-fibrosis-cf/life-expectancy

9. Jackson AD, Goss CH. Epidemiology of CF: How registries can be used to advance our understanding of the CF population. J Cyst Fibros. 2018;17(3):297–305.

10. Elborn JS. Adult Care in Cystic Fibrosis. Semin Respir Crit Care Med. 2019;40(6):857–68.

11. Nazareth D, Walshaw M. A review of renal disease in cystic fibrosis. J Cyst Fibros [Internet]. 2013;12(4):309–17. Available from: http://dx.doi.org/10.1016/j.jcf.2013.03.005

12. Death E. Chronic Kidney Disease in the United States , 2021. 2021;

13. Phe K, Lee Y, McDaneld PM, Prasad N, Yin T, Figueroa DA, et al. In vitro assessment and multicenter cohort study of comparative nephrotoxicity rates associated with colistimethate versus polymyxin b therapy. Antimicrob Agents Chemother. 2014;58(5):2740–6.

14. Crass RL, Rutter WC, Burgess DR, Martin CA, Burgess DS. Nephrotoxicity in patients with or without cystic fibrosis treated with Polymyxin B compared to colistin. Antimicrob Agents Chemother. 2017;61(4):1–11.

15. Novel-Catin E, Pelletier S, Reynaud Q, Nove-Josserand R, Durupt S, Dubourg L, et al. Aminoglycoside exposure and renal function before lung transplantation in adult cystic fibrosis patients. Nephrol Dial Transplant. 2019;34(1):118–22.

16. Corradi V, Vergani P, Tieleman DP. Cystic fibrosis transmembrane conductance regulator (CFTR):closedandopenstate channelmodels. J Biol Chem [Internet]. 2015;290(38):22891–906. Available from: http://dx.doi.org/10.1074/jbc.M115.665125

17. Ratjen F, Bell SC, Rowe SM, Goss CH, Quittner AL, Bush A. Cystic fibrosis. Nat Rev Dis Prim [Internet]. 2015;1(May):1–19. Available from: http://dx.doi.org/10.1038/nrdp.2015.10

18. Marson FAL, Bertuzzo CS, Ribeiro JD. Classification of CFTR mutation classes. Lancet Respir Med. 2016;4(8):e37–8.

19. Nielsen R, Christensen EI, Birn H. Megalin and cubilin in proximal tubule protein reabsorption: From experimental models to human disease. Kidney Int [Internet]. 2016;89(1):58–67. Available from: http://dx.doi.org/10.1016/j.kint.2015.11.007

20. Vandewalle A, Farman N, Morin JP, Fillastre JP, Hatt PY, Bonvalet JP. Gentamicin incorporation along the nephron: Autoradiographic study on isolated tubules. Kidney Int. 1981;19(4):529–39.

21. Azad MAK, Finnin BA, Poudyal A, Davis K, Li J, Li J, et al. Polymyxin B induces apoptosis in kidney proximal tubular cells. Antimicrob Agents Chemother. 2013;57(9):4329–35.

22. Mahadevappa R, Nielsen R, Christensen EI, Birn H. Megalin in acute kidney injury: Foe and friend. Am J Physiol - Ren Physiol. 2014;306(2):147–54.

23. Jouret F, Bernard A, Hermans C, Dom G, Terryn S, Leal T, et al. Cystic fibrosis is associated with a defect in apical receptor-mediated endocytosis in mouse and human kidney. J Am Soc Nephrol. 2007;18(3):707–18.

24. Zhang Y, Fang X, Xu H, Shen Q. Genetic analysis of dent's disease and functional

research of CLCN5 mutations. DNA Cell Biol. 2017;36(12):1151–8.

25. Gruenert DC, Willems M, Cassiman JJ, Frizzell RA. Established cell lines used in cystic fibrosis research. J Cyst Fibros. 2004;3(SUPPL. 2):191–6.

26. Sun X, Meyerholz DK, Engelhardt JF, Sun X, Sui H, Fisher JT, et al. Disease phenotype of a ferret CFTR -knockout model of cystic fibrosis Find the latest version : Technical advance Disease phenotype of a ferret CFTR -knockout model of cystic fibrosis. J Clin Invest. 2010;120(9):3149–60.

27. Semaniakou A, Croll RP, Chappe V. Animal Models in the Pathophysiology of Cystic Fibrosis. Front Pharmacol [Internet]. 2019 Jan 4;9(JAN):1–16. Available from: https://www.frontiersin.org/article/10.3389/fphar.2018.01475/full

28. Ashammakhi N, Darabi MA, Çelebi-Saltik B, Tutar R, Hartel MC, Lee J, et al. Microphysiological Systems: Next Generation Systems for Assessing Toxicity and Therapeutic Effects of Nanomaterials. Small Methods. 2020;4(1):1–19.

29. Diekjürgen D, Grainger DW. Drug transporter expression profiling in a three-dimensional kidney proximal tubule in vitro nephrotoxicity model. Pflugers Arch Eur J Physiol. 2018;470(9):1311–23.

30. Weber EJ, Chapron A, Chapron BD, Voellinger JL, Lidberg KA, Yeung CK, et al. Development of a microphysiological model of human kidney proximal tubule function. Kidney Int [Internet]. 2016;90(3):627–37. Available from: http://dx.doi.org/10.1016/j.kint.2016.06.011

31. Sakolish C, Weber EJ, Kelly EJ, Himmelfarb J, Mouneimne R, Grimm FA, et al. Technology Transfer of the Microphysiological Systems: A Case Study of the Human Proximal Tubule Tissue Chip. Sci Rep [Internet]. 2018;8(1):1–14. Available from: http://dx.doi.org/10.1038/s41598-018-33099-2

32. Yu M, Sun X, Tyler SR, Liang B, Swatek AM, Lynch TJ, et al. Highly Efficient Transgenesis in Ferrets Using CRISPR/Cas9-Mediated Homology-Independent Insertion at the ROSA26 Locus. Sci Rep. 2019;9(1):1–13.

33. Imaoka T, Yang J, Wang L, McDonald MG, Afsharinejad Z, Bammler TK, et al. Microphysiological system modeling of ochratoxin A-associated nephrotoxicity. Toxicology [Internet]. 2020;444(July):1–10. Available from: https://doi.org/10.1016/j.tox.2020.152582

34. Weber EJ, Lidberg KA, Wang L, Bammler TK, MacDonald JW, Li MJ, et al. Human kidney on a chip assessment of polymyxin antibiotic nephrotoxicity. JCI insight. 2018;3(24):1–17.

35. Lidberg KA, Annalora AJ, Jozic M, Elson DJ, Wang L, Bammler TK, et al. Antisense oligonucleotide development for the selective modulation of CYP3A5 in renal disease. Sci Rep [Internet]. 2021;11(1):1–20. Available from: https://doi.org/10.1038/s41598-021-84194-w

36. Wilmer MJ, Saleem MA, Masereeuw R, Ni L, Van Der Velden TJ, Russel FG, et al. Novel conditionally immortalized human proximal tubule cell line expressing functional influx and efflux transporters. Cell Tissue Res. 2010;339(2):449–57.

37. Tobergte DR, Curtis S. measurement of GFR included kidney research experimental protocols. Vol. 53, Journal of Chemical Information and Modeling. 2013. 1689–1699 p.

38. Sánchez-Romero N, Martínez-Gimeno L, Caetano-Pinto P, Saez B, Sánchez-Zalabardo JM, Masereeuw R, et al. A simple method for the isolation and detailed characterization of primary human proximal tubule cells for renal replacement therapy. Int J Artif Organs. 2020;43(1):45–57.

39. Qi W, Johnson DW, Vesey DA, Pollock CA, Chen X. Isolation, propagation and characterization of primary tubule cell culture from human kidney (Methods in Renal Research). Nephrology. 2007;12(2):155–9.

40. Ding W, Yousefi K, Shehadeh LA. Isolation, characterization, and high throughput extracellular flux analysis of mouse primary renal tubular epithelial cells. J Vis Exp. 2018;2018(136):1–10.

41. Aresu L, Rastaldi MP, Scanziani E, Baily J, Radaelli E, Pregel P, et al. Epithelial-mesenchymal transition (EMT) of renal tubular cells in canine glomerulonephritis. Virchows Arch. 2007;451(5):937–42.

42. He T, Guan X, Wang S, Xiao T, Yang K, Xu X, et al. Resveratrol prevents high glucose-induced epithelial-mesenchymal transition in renal tubular epithelial cells by inhibiting NADPH oxidase/ROS/ERK pathway. Mol Cell Endocrinol [Internet]. 2015;402:13–20. Available from: http://dx.doi.org/10.1016/j.mce.2014.12.010

43. Dare E V., Griffith M, Poitras P, Kaupp JA, Waldman SD, Carlsson DJ, et al. Genipin

cross-linked fibrin hydrogels for in vitro human articular cartilage tissue-engineered regeneration. Cells Tissues Organs. 2009;190(6):313–25.

44. Sasaki H, Sugiyama M, Sasaki N. Establishment of renal proximal tubule cell lines derived from the kidney of p53 knockout mice. Cytotechnology [Internet]. 2019;71(1):45–56. Available from: https://doi.org/10.1007/s10616-018-0261-1

45. Devesa P, Agasse F, Xapelli S, Almengló C, Devesa J, Malva JO, et al. Growth hormone pathways signaling for cell proliferation and survival in hippocampal neural precursors from postnatal mice. BMC Neurosci. 2014;15(1–11).

46. Ledda-Columbano GM, Perra A, Loi R, Shinozuka H, Columbano A. Cell proliferation induced by triiodothyronine in rat liver is associated with nodule regression and reduction of hepatocellular carcinomas. Cancer Res. 2000;60(3):603–9.

47. Liu Y, Yu X, Zhuang J. Epinephrine Stimulates Cell Proliferation and Induces Chemoresistance in Myeloma Cells through the β-Adrenoreceptor in vitro. Acta Haematol. 2017;138(2):103–10.

48. Jászai J, Farkas LM, Fargeas CA, Janich P, Haase M, Huttner WB, et al. Prominin-2 is a novel marker of distal tubules and collecting ducts of the human and murine kidney. Histochem Cell Biol. 2010;133(5):527–39.

49. Olea-Flores M, Juárez-Cruz JC, Zuñiga-Eulogio MD, Acosta E, García-Rodríguez E, Zacapala-Gomez AE, et al. New actors driving the epithelial–mesenchymal transition in cancer: The role of leptin. Biomolecules. 2020;10(12):1–29.

50. Hertig A. Epithelial-mesenchymal transition of the renal graft. Nephrol Ther. 2008;4:25–8.

51. Weigmann B, Tubbe I, Seidel D, Nicolaev A, Becker C, Neurath MF. Isolation and subsequent analysis of murine lamina propria mononuclear cells from colonic tissue. Nat Protoc. 2007;2(10):2307–11.

52. Chandrasekaran V, Carta G, da Costa Pereira D, Gupta R, Murphy C, Feifel E, et al. Generation and characterization of iPSC-derived renal proximal tubule-like cells with extended stability. Sci Rep [Internet]. 2021;11(1):1–17. Available from: https://doi.org/10.1038/s41598-021-89550-4

53. Xia S, Wu M, Chen S, Zhang T, Ye L, Liu J, et al. Long Term Culture of Human Kidney Proximal Tubule Epithelial Cells Maintains Lineage Functions and Serves as an Ex vivo Model for Coronavirus Associated Kidney Injury. Virol Sin [Internet]. 2020;35(3):311–20. Available from: https://doi.org/10.1007/s12250-020-00253-y

54. Liu X, Krawczyk E, Suprynowicz FA, Palechor-Ceron N, Yuan H, Dakic A, et al. Conditional reprogramming and long-term expansion of normal and tumor cells from human biospecimens. Nat Protoc. 2017;12(2):439–51.

55. Jeong SY, Lee JH, Shin Y, Chung S, Kuh HJ. Co-culture of tumor spheroids and fibroblasts in a collagen matrix-incorporated microfluidic chip mimics reciprocal activation in solid tumor microenvironment. PLoS One. 2016;11(7):1–17.

56. Sheppard DN, Welsh MJ. Structure and function of the CFTR chloride channel. Physiol

Rev. 1999;79(1 SUPPL. 1):23–45.